PHOTOGRAPH THIS SHEET

POR-2000(EX)
OPERATION DOMINIC, SHOT SWORD FISH

LEVEL

7

INVENTORY

AD-A995 472

DTIC ACCESSION NUMBER

25 June 1968

DOCUMENT IDENTIFICATION

DISTRIBUTION STATEMENT A
Approved for public release;
Distribution Unlimited

DISTRIBUTION STATEMENT

ACCESSION FOR		
NTIS	GRA&I	☑
DTIC	TAB	☐
UNANNOUNCED		☐
JUSTIFICATION		
BY		
DISTRIBUTION /		
AVAILABILITY CODES		
DIST	AVAIL AND/OR SPECIAL	
A-1		

DISTRIBUTION STAMP

DTIC COPY INSPECTED

DTIC
ELECTE
MAY 26 1987
S D
D

DATE ACCESSIONED

UNANNOUNCED

DATE RETURNED

87 5 19 133

DATE RECEIVED IN DTIC

REGISTERED OR CERTIFIED NO.

PHOTOGRAPH THIS SHEET AND RETURN TO DTIC-FDAC

DTIC FORM 70A
MAR 86

DOCUMENT PROCESSING SHEET

PREVIOUS EDITION MAY BE USED UNTIL STOCK IS EXHAUSTED.

POR-2000(EX)
(WT-2000)(EX)
EXTRACTED VERSION

OPERATION DOMINIC, SHOT SWORD FISH

Project Officer's Report—Project 1.1
Underwater Pressures

Robert S. Price, Project Officer
Daniel J. Torpy
Valmore F. DeVost
Larry W. Bell
U.S. Naval Ordnance Laboratory
White Oak
Silver Spring, MD 20910

25 June 1968

NOTICE:
This is an extract of POR-2000, Operation DOMINIC, Shot Sword Fish, Project 1.1.

Extracted version prepared for
Director
DEFENSE NUCLEAR AGENCY
Washington, DC 20305-1000

1 September 1985

Destroy this report when it is no longer needed. Do not return to sender.

PLEASE NOTIFY THE DEFENSE NUCLEAR AGENCY, ATTN: STTI, WASHINGTON, DC 20305-1000, IF YOUR ADDRESS IS INCORRECT, IF YOU WISH IT DELETED FROM THE DISTRIBUTION LIST, OR IF THE ADDRESSEE IS NO LONGER EMPLOYED BY YOUR ORGANIZATION.

UNCLASSIFIED
SECURITY CLASSIFICATION OF THIS PAGE

AD-A995 477

REPORT DOCUMENTATION PAGE

1a. REPORT SECURITY CLASSIFICATION UNCLASSIFIED	1b. RESTRICTIVE MARKINGS
2a. SECURITY CLASSIFICATION AUTHORITY	3. DISTRIBUTION / AVAILABILITY OF REPORT Approved for public release; distribution is unlimited.
2b. DECLASSIFICATION / DOWNGRADING SCHEDULE	
4 PERFORMING ORGANIZATION REPORT NUMBER(S)	5. MONITORING ORGANIZATION REPORT NUMBER(S) POR-2000 (EX) (WT-2000 (EX))
6a. NAME OF PERFORMING ORGANIZATION U.S. Naval Ordnance Laboratory 6b OFFICE SYMBOL (If applicable)	7a. NAME OF MONITORING ORGANIZATION Defense Atomic Support Agency
6c. ADDRESS (City, State, and ZIP Code) White Oak, MD	7b. ADDRESS (City, State, and ZIP Code) Washington, DC
8a. NAME OF FUNDING / SPONSORING ORGANIZATION 8b. OFFICE SYMBOL (If applicable)	9. PROCUREMENT INSTRUMENT IDENTIFICATION NUMBER
8c. ADDRESS (City, State, and ZIP Code)	10 SOURCE OF FUNDING NUMBERS PROGRAM ELEMENT NO. / PROJECT NO. / TASK NO. / WORK UNIT ACCESSION NO.

11 TITLE (Include Security Classification) OPERATION DOMINIC, SHOT SWORD FISH, PROJECT OFFICERS REPORT - Project 1.1 - Underwater Pressures, Extracted Version

12 PERSONAL AUTHOR(S)
R.S. Price, D.J. Torpy, V.F. DeVost and L.W. Bell

13a TYPE OF REPORT	13b TIME COVERED FROM ____ TO ____	14 DATE OF REPORT (Year, Month, Day)	15 PAGE COUNT
		680625	

16 SUPPLEMENTARY NOTATION This report has had sensitive military information removed in order to provide an unclassified version for unlimited distribution. The work was performed by the Defense Nuclear Agency in support of the DoD Nuclear Test Personnel Review Program.

17 COSATI CODES		
FIELD	GROUP	SUB-GROUP
18	3	
19	4	

18. SUBJECT TERMS (Continue on reverse if necessary and identify by block number)
Dominic, Sword Fish, Underwater Explosions, Hydrodynamic Yield, Depth of Burst, Dynamic Pressure

19 ABSTRACT (Continue on reverse if necessary and identify by block number)

The objectives of this project were to: (1) determine the Sword Fish hydrodynamic yield, depth of burst, time of burst, and surface zero position; (2) determine the effect of reflection and refraction on the dynamic pressures; and (3) deduce the Sword Fish burst bubble history. These were accomplished by making underwater dynamic pressure measurements.

20 DISTRIBUTION / AVAILABILITY OF ABSTRACT ☒ UNCLASSIFIED/UNLIMITED ☐ SAME AS RPT ☐ DTIC USERS	21. ABSTRACT SECURITY CLASSIFICATION UNCLASSIFIED
22a. NAME OF RESPONSIBLE INDIVIDUAL Mark D. Flohr	22b TELEPHONE (Include Area Code) 202-325-7759 22c. OFFICE SYMBOL DNA/ISCM

DD FORM 1473, 84 MAR 83 APR edition may be used until exhausted. All other editions are obsolete.

SECURITY CLASSIFICATION OF THIS PAGE
UNCLASSIFIED

OPERATION DOMINIC

SHOT SWORD FISH

PROJECT OFFICERS REPORT—PROJECT 1.1

UNDERWATER PRESSURES (U)

Robert S. Price, Project Officer
Daniel J. Torpy,
Valmore F. DeVost
Larry W. Bell

U. S. Naval Ordnance Laboratory
White Oak
Silver Spring, Maryland 20910

ABSTRACT

Project objectives were to: (1) determine the Sword Fish hydrodynamic yield, depth of burst, time of burst, and surface zero position; (2) determine the effects of reflection and refraction on the dynamic pressures; and (3) deduce the Sword Fish burst bubble history.

Measurements of the underwater dynamic pressures, using piezoelectric pressure-time gages and magnetic-tape recorders, were made at five stations at horizontal ranges from 3,100 to 20,250 feet. Gage depths varied from 20 to 2,000 feet. Ball crusher peak-pressure gages were used as backups at three close-in stations at gage depths from 25 to 1,000 feet. Time-of-arrival data was recorded at one station at a range of 23,800 feet. Ninety-four percent of the tape records and ninety-one percent of the ball crusher records yielded usable data.

The results of the shot, fired under the particular conditions of Sword Fish, were as follows:

1. The hydrodynamic yield was found to be equivalent to The depth of burst was 690 ± 10 feet. The time of burst was calculated to be 2002:05:909 ± .005 GMT, 11 May 1962, about 39.809 seconds after the launch (zero) time. Geographical surface zero position was not determined by the project.

2. Refraction effects were detected in electronic pressure measurements at ranges of over 4,000 feet. Mechanical gages showed refraction effects even as close in as 3,120 feet.

3. No bubble pulse was detected.

4. The bottom reflection, at ranges over 6,400 feet, was stronger than the direct wave.

Computer codes especially developed for this situation were employed in the analysis; they are adaptable for the analysis of future test results.

PREFACE

Shot Sword Fish was an underwater weapon effects test conducted in the Pacific Ocean off the southwest coast of the United States in May 1962 as part of Operation Dominic. Sword Fish was the first fully operational test of the Navy's antisubmarine rocket (ASROC) weapon system in which a nuclear war reserve weapon was expended. Weapon effects information of importance to the advancement of surface ship capability to conduct nuclear antisubmarine warfare was obtained. An overall description of the test efforts and a summary of preliminary results may be found in the Sword Fish Scientific Director's Summary Report, which includes general information such as location and time of burst and a guide to Sword Fish reports (Reference 18).

CONTENTS

ABSTRACT ---------- 5

PREFACE ---------- 7

CHAPTER 1 INTRODUCTION ---------- 13

1.1 Objectives ---------- 13
1.2 Background and Theory ---------- 13

CHAPTER 2 PROCEDURE ---------- 16

2.1 Experimental Arrangements ---------- 16
2.2 Instrumentation ---------- 18
2.2.1 Ball Crusher Gages ---------- 18
2.2.2 Tourmaline Gages ---------- 24
2.2.3 Lead Zirconate Hydrophones ---------- 28
2.2.4 Electrical Recording Equipment ---------- 29
2.2.5 The Playback System ---------- 35
2.2.6 Electronic Pressure-Time Record Analysis ---------- 35
2.2.7 Mechanized Data Analysis ---------- 37
2.2.8 Mechanical Support and Rigging ---------- 39
2.3 Preshot Operations ---------- 42
2.4 Shot Operations ---------- 43
2.5 Postshot Operations ---------- 46
2.6 Computations of Shock Arrival Times ---------- 46

CHAPTER 3 RESULTS ---------- 66

3.1 Records and Measurements ---------- 66
3.1.1 Event Time on EPT Records ---------- 67
3.1.2 Pressure Measurements, BC Gages ---------- 68
3.1.3 Pressure Measurements, Electronically Recorded ---------- 70
3.1.4 Time Constant, θ ---------- 71
3.1.5 Impulse and Energy Flux Measurements ---------- 72
3.2 Data From Other Projects ---------- 73
3.2.1 Photographic Data ---------- 73
3.2.2 Shock Wave Arrival Times ---------- 73
3.2.3 Hydrographic Data ---------- 74

CHAPTER 4 DISCUSSION ---------- 106

4.1 Location of Burst ---------- 106
4.2 Time of Burst ---------- 111
4.3 Refraction Effects ---------- 112
4.4 Yield Calculations ---------- 115
4.5 Other Phenomena ---------- 119

CHAPTER 5 CONCLUSIONS ---------- 139

APPENDIX MECHANICAL SHOCK MEASUREMENTS ---------- 140

A.1 NOL Copper Ball Accelerometers ---------- 140
A.2 Accelerometer Mounts ---------- 141
A.3 Results ---------- 142

REFERENCES ---------- 145

TABLES

2.1 Instrumentation Data for Each Instrumented Point ---------- 51
2.2 Calibration Data for Tourmaline Gages ---------- 53
2.3 Hydrophone Calibrations at Station 4 ---------- 54
2.4 Time Base Data ---------- 55
2.5 Comparison of Data Reduction Systems ---------- 56
3.1 Summary of Sword Fish Recordings ---------- 75
3.2 Times of Arrival of Pulses at Piezoelectric Gages ---------- 77
3.3 Ball Measurements and Pressure Values for Ball Crusher Gages at Station 1 ---------- 79
3.4 Ball Measurements and Pressure Values for Ball Crusher Gages at Station 2 ---------- 87
3.5 Ball Measurements and Pressure Values for Ball Crusher Gages at Station 3 ---------- 92
3.6 Pressure Measurements, Electronically Recorded ---------- 97
3.7 Time Constant, θ, and Extrapolated Peak Pressure ---------- 98
3.8 Impulse, I, and Energy Flux, E ---------- 99
3.9 Location of Gage Strings Relative to Surface Zero at Time of Burst From Photographic Measurements ---------- 100
3.10 Time of Arrival of Shock Wave at Project 3.1 Velocity Meters ---------- 101
3.11 Depth Versus Computed Sound Velocity ---------- 102
4.1 Depths of Burst Calculated by Matching Various Parameters ---------- 123
4.2 Depth of Burst Determination From Averages ---------- 124

4.3 Depth of Burst Determination, Final Computations ---------- 125
4.4 Yield From Ball Crusher Peak Pressures ---------- 126
4.5 Yield Based on Shock Wave Parameters (Hand Measurements and Machine Computations) ---------- 130
4.6 Yield Based on Shock Wave Parameters (Machine Computations and Extrapolations) ---------- 131
4.7 Bottom Depths Postulated on Basis of Bottom Reflection Arrival Times ---------- 132
4.8 Bottom Reflection Characteristics ---------- 133

FIGURES

2.1 Planned locations of pressure-measuring stations ---------- 57
2.2 Actual deduced locations of pressure-measuring stations ---------- 58
2.3 Dynamic force coefficients, copper balls ---------- 59
2.4 Initial ball deformation and the hydrostatic pressure correction term, copper balls ---------- 60
2.5 Dynamic calibration shock waves ---------- 61
2.6 Schematic of calibration and data signals during playback ---------- 62
2.7 Comparison of manual and mechanical record reading ---------- 63
2.8 Instrument container at Stations 1 and 2 ---------- 64
2.9 Installation of PE and BC gages ---------- 65
3.1 Electronic pressure-time record, unrefracted ---------- 103
3.2 Electronic pressure-time record, refracted ---------- 104
3.3 Sound velocity versus depth at test site ---------- 105
4.1 Results of depth of burst calculations ---------- 134
4.2 Ball crusher peak pressures versus depth ---------- 135
4.3 Sound ray paths ---------- 136
4.4 Isointensity contours ---------- 137
4.5 Intensity factor versus depth at three stations ---------- 138
A.1 Accelerometer arrangements ---------- 144

CHAPTER 1

INTRODUCTION

1.1 OBJECTIVES

The objectives of Project 1.1 were to: (1) determine the Sword Fish hydrodynamic yield, depth of burst, time of burst, and surface zero position ; (2) determine the effect of reflection and refraction on the dynamic pressures; and (3) deduce the Sword Fish burst bubble history. These were to be accomplished by making underwater dynamic pressure measurements.

1.2 BACKGROUND AND THEORY

Data from two previous underwater nuclear explosions in deep water are available. Operation Wigwam (References 1, 2, and 3) provided basic information for comparing nuclear and high explosives under water. Refraction effects on the shock wave, evidence of a condensing bubble (Reference 2), bottom reflections of the shock wave, and cavitation closure pulses were reported. Wigwam data was the only deep water information available for establishing operational conditions for the application of nuclear weapons. Because of the

complexity of the various explosion effects and their interactions with the hull and equipment of ships, Shot Wahoo was fired during Operation Hardtack to verify predicted effects upon target vessels. Test conditions were arranged to facilitate measurement of bottom reflection, cavitation closure, and primary shock wave effects on ship targets. The selected site was over a sloping bottom, and the weapon was suspended at a preset depth.

Many of the desired records of underwater pressure (References 4 and 5) were not obtained from Shot Wahoo because of malfunctioning equipment and operational losses. Records were not obtained at enough locations to permit more refined refraction predictions or to improve understanding of the cavitation closure phenomena. No bubble pulse was detected on the records; however, since the bubble would have migrated to a position very close to the ocean's surface before emitting the pulse, the pulse, if it did occur, might have been masked by surface cutoff (reflection as a negative pressure wave from a free surface). The importance of the primary shock wave after reflection from the ocean bottom, especially if focusing has occurred, was brought out during Operation Wigwam. Shot Wahoo was fired under conditions of bottom depth and contour that produced reflection effects on target vessels; however, the conditions were unfavorable for producing significant focusing effects, and none were reported.

Sword Fish was intended to provide results for comparison with Wigwam free-field measurements, provide a full-scale refraction effect for comparison with laboratory and theoretical work, permit further study of bulk-cavitation closure, and provide bottom-reflected shock wave characteristics.

The Sword Fish bubble pulse was expected to be difficult to measure because, as for Wahoo, the bubble would have migrated to a shallow depth before completing its first oscillation. For Wigwam the approximate time of maximum contraction was indicated by a sharp-fronted wave imposed upon the normal rounded bubble pulse. The sharp-fronted wave was attributed to the impact of the top and bottom of the bubble during the beginning of vortical motion. A similar sharp wave or perhaps multiple sharp waves were expected from the Sword Fish bubble. In the absence of such waves, source location and perhaps even detection of the rounded pulse would be impossible, and this result would be taken as evidence that the bubble had not collapsed as expected.

CHAPTER 2

PROCEDURE

2.1 EXPERIMENTAL ARRANGEMENTS

Figure 2.1 shows the planned locations, relative to the target float, of the five stations at which underwater pressure measurements were to be made. Figure 2.2 shows the actual location of surface zero and the instrument stations at shot time, as deduced from aerial photographs, shock wave arrival times, and radar plots.

Table 2.1 lists the planned gage depth, type, and size for each of the six stations. The data from the electronic pressure-time (EPT) gages at five stations was recorded on magnetic tape in recorders which were originally built for Hardtack and extensively modified for use on Sword Fish. The recorder at Station 6 was a Sony Sterecorder, Model 464D. One recorder was located at each station. For all stations, generally uniform spacing of gages was decided upon, since the effects of refraction and any unexpected phenomena could be detected better than if lump placement of gages at two or three depths had been used. The latter arrangement would only have checked the accuracy of the gage and recording system and assured data from one specific point in case of

failure of a single gage. More closely spaced gages at shallow depths were used when more information in that region was deemed vital.

Data from Stations 1 and 2 were to be used primarily in determining the depth of burst, yield, bubble period, and bubble migration. Secondarily, they would provide information on the bulk cavitation closure and the bottom reflection. It was judged that the value of data would rapidly degenerate for the primary purposes as the horizontal range increased. The two stations were mutual backups to allow for normal dispersion in projection placement of weapons. Station 1 would be better if the burst were more remote than expected; Station 2 should have recorded and survived if the burst were near enough to just sink Station 1. The deep gages would produce records least distorted by surface cutoff and refraction effects and, with the shallow gages, would provide long baselines for depth-of-burst and bubble-migration measurements. Data from Station 3 was primarily to provide exact free-field pressure input to the towed target vessel for shock and damage evaluation. Information on refraction would also be obtained. Station 4 was to provide data on refraction effects and the bottom reflection as well as shock input data to the towing vessel. Station 5 was to provide shock input data to the delivery vessel, or, if a change in delivery vessel was

necessary, to an equivalent vessel similarly situated relative to the explosion. Station 6 was to provide arrival-time data at a rather remote location.

2.2 INSTRUMENTATION

Most recording instrumentation used for Sword Fish had been used for Operation Hardtack except that, where time permitted, modifications were made to improve reliability and to facilitate use in the field. Replacement and new parts selected for use on Sword Fish are described below; equipment not altered or redesigned is mentioned for identification, and further description can be found in Reference 5.

2.2.1 Ball Crusher Gages. Ball crusher (BC) gages have been used for many years to measure the peak pressure from underwater explosions. Pressure, transmitted through a piston, presses a soft copper ball against an anvil, causing a permanent deformation of the ball. The amount of deformation is a function of the hydrostatic pressure at the gage location, the shock wave peak pressure, the time constant of the subsequent pressure decay, the area of the piston, the mass of the piston, the mass of the gage, and the particular properties of the copper sphere that was used. The design of the BC gage with O-ring seals as used on Sword Fish is described in detail in Reference 5.

Instead of using four gages per block as described in Reference 5, three gages were mounted on a block, and the fourth mounting hole was used for attaching either a piezoelectric gage bracket or a bracket to hold the electric cables. Blocks were placed at 25-foot spacing at depths from 25 to 1,000 feet at Stations 1, 2, and 3. Two sizes of ball were used: 3/8-inch diameter for expected pressures over 700 psi and 5/32-inch diameter for expected pressures from 300 to 1,500 psi. Station 2 was expected to be in the region of overlap between 700 and 1,500 psi, so both ball sizes were used there. Blocks carrying gages with 3/8-inch-diameter balls were alternated on the support cable with blocks carrying gages with 5/32-inch-diameter balls.

Balls are usually calibrated by dropping weights on them and also by slowly loading them with a known force to determine calibration constants for conversion of deformation readings to pressure. Thus, two separate calibrations are made for each group (or lot) of balls.

One equation for converting deformation readings to shock wave pressure (assuming that the time constant of the shock wave is very long compared to the reaction time of the gage) is:

$$P = \frac{K_d X_m}{24A} + \frac{K_d X_o}{24A} - P_o \qquad (2.1)$$

Where: P = the shock pressure, psi

K_d = the dynamic force "constant", pounds per foot

X_m = the final, measured deformation, inches

A = the area of the piston, square inches (0.196 for Sword Fish gages)

X_o = the initial deformation caused by the hydrostatic pressure, inches

P_o = the hydrostatic pressure, psi; it is equal to about $0.444\ D_o$

D_o = the depth to which the gage is lowered, feet.

The dynamic force constant is defined by:

$$K_d = \frac{2E}{\Delta^2} \qquad (2.2)$$

Where: E = energy dissipated in deforming a ball, foot-pounds

Δ = permanent deformation of the ball, feet

The constant, K_d, is determined for each ball size by dropping various carefully weighed steel bars through measured distances onto balls located on an anvil. The equipment is described in Reference 6. The weights used prior to 1962 had been lost, so new ones were manufactured and weighed before use.

Usually, a plot of the square root of the energy versus deformation was constructed. A best straight line was then drawn through the calibration data points and the slope of

this line used to determine K_d. The line may not have passed through the origin of the graph. In analyzing the Sword Fish records, which had relatively small deformations, it was found that the assumption of a constant K_d was inadequate. (Also when the deformation is very large, the assumption is not adequate, see Reference 7.) Instead, the ratio of twice the energy to the deformation squared (K_d by definition) as determined from the calibration drops for each measured deformation, X_m, was used. The values of K_d are shown in Figure 2.3 and obviously are not constant with deformation; therefore, K_d should properly be referred to as the "dynamic force coefficient" rather than "dynamic force constant".

The value of the initial ball deformation, X_o, in Equation 2.1 has usually been calculated on the assumption that it is a linear function of the hydrostatic pressure. The equation is:

$$X_o = 12 \frac{(0.444\ D_o\ A)}{K_s} \qquad (2.3)$$

in which K_s is a static force constant in pounds per foot. K_s was determined from data obtained by placing groups of assembled gages in a pressure chamber and slowly raising the pressure to a measured value (Reference 2). After pressure release, the gages were removed, and other groups were loaded to other pressure values. Since the process was cumbersome,

relatively few pressure levels were used. The measured deformations were then plotted as a function of the applied force. The slope of the best straight line through the points determined K_s. It was known that the true line was not straight.

After Sword Fish, new static calibrations were performed using a different method. Balls were deformed by pressing them against an anvil placed on the table of a platform scale. A nonrotating, screw-actuated plunger was used to apply the force. The resulting deformations and those produced by hydraulic loading of assembled gages were found to be comparable.

The use of a platform scale as a force-measuring device was not entirely satisfactory in that balance-type scales have maximum sensitivity when the system is oscillating slowly about the balance point and the indicator point is oscillating slowly past the scale index line. When essentially loaded by an inelastic jack load, the sensitivity is greatly decreased. However, with slow application of the load and careful centering of the indicator point on the scale index line, the observed sensitivity of the balance used was found to be adequate for ball-deformation calibration use. Because of the convenience of operation, the platform balance did make possible easy acquisition of deformation readings at numerous load levels.

It was noticed, as has been observed in calibrations over the past 10 or 15 years, that deformation was not a

linear function of the force. The data are shown in Figure 2.4, and the difference between the response of the two ball sizes is remarkable. The previous data had been too sparse to show the effects revealed here.

Because of this evidence, it was decided to use values of X_o obtained from the calibration data rather than values calculated from a linear function.

Since X_o (certainly for the 3/8-inch-diameter balls, and perhaps for the 5/32-inch-diameter balls) becomes zero at a finite depth, it has been assumed in the Sword Fish data analysis that P_o also becomes zero at the same finite depth. This assumption is in turn based on the assumptions that both X_o and P_o are used together in the hydrostatic correction and that elastic deformation that does not produce a flat on a ball does not affect subsequent dynamic deformation. Though these assumptions are unproved, the fit of the data at Station 2, where two ball sizes were used, does not disprove them. At depths of 200 to 300 feet, the hydrostatic response of the large and small balls are markedly different, and incorrect application of hydrostatic corrections should cause the pressure values derived from the two ball sizes to be more divergent than is apparent (see Figure 4.2).

The use of nonlinear calibration curves was found to be essential to give consistent results in analyzing the Sword Fish data; it is unfortunate that such curves were not more frequently used in the past.

2.2.2 Tourmaline Gages. Tourmaline piezoelectric pressure-time gages (PE) of the types used during Operation Hardtack were used. The size of gage used at each place was determined by the capacitance of the cable connecting the gage to the recorder, the predicted pressure at the gage location, the time constant of the recording system desired, the capacitance in the cable termination unit, the combination of leakage and input resistances, and the voltage desired at the recorder input. Gages were statically calibrated (Reference 2). After mounting on cable (0.270-inch O.D. antimicrophonic cable manufactured by Simplex Wire & Cable Co.), they were exposed to the underwater shock waves from two detonators to reduce the first-time gage effect (Reference 8). All gages and their attached cables were tested hydrostatically to check the watertightness of the cable jacket and gage coating. No dynamic calibrations were made prior to the operation.

After the field phase of Sword Fish was concluded, 23 of the 28 tourmaline gages used were statically recalibrated on their cables at 100, 300, and 500 psi. The other five could not be calibrated, as used, because of low resistance or open leads. Two were remounted and subsequently recalibrated. These calibrations are given in Table 2.2.

Eighteen dynamic calibration shots were then fired, and 198 records (including those from hydrophones) were obtained.

Three sizes of tapered line charge were used to obtain step shock waves of 450-to 900-μsec duration with plateau pressure levels ranging from 110 to 1,320 psi. Measurements were made off the small end of the charge, where detonation was started, at distances ranging from 2 to 25 feet. Charges weighing 4 and 9 pounds were cast of 50/50 pentolite in metal tubes which were left in place as a permanent casing. Bare charges weighing 5 pounds were cast of 50/50 pentolite in a reusable metal mold. The above charges were 48, 54, and 27 inches long, respectively.

Five 1/4-inch-diameter, four element, wax-coated gages (the type used in underwater tests of high explosives by the Underwater Explosions Division of the Naval Ordnance Laboratory (NOL)) were used as "standards". They determined the pressures in the calibration shock waves as they would be measured in a conventional high explosive comparison series. No more than four of these gages were used on any shot; the fifth gage was either under repair or held in reserve.

Shock waves measured by one standard gage at three pressure levels are shown in Figure 2.5. The records are fairly typical of those obtained using standard gages. Also shown are comparable records obtained by 1/2-inch, 1-1/8-inch (four pile), and 2-inch tourmaline gages used on Sword Fish.

The effect of gage size is particularly evident in the

smoothing of small irregularities on the shock wave and the longer rise time when recorded by a 2-inch gage. It is because of these effects that the tapered charge, rather than a spherical one, is used in dynamic calibration shots. Even so, the comparison of pressure levels is not clear cut. The height of a straight line through a portion of the pressure-time curve at a selected time after the mid-point of the initial rise was used to determine the response of the specimen gage. The pressure was measured similarly on the standard gage records. The gage constant (KA, μcoulombs/psi) for the specimen gage was then calculated using the measured pressure, known circuit constants, and system calibration (Reference 9). Measurements of impulse and independent measurements of pressure by different people yielded comparable values.

At first, gages were placed at distances such that the plateau pressure in the calibration shock wave was comparable to the peak pressure measured on Sword Fish. Later, gages were placed at other ranges to determine their output linearity as a function of pressure.

The results from the tests were most discouraging. The standard gages did not yield reproducible results--on one shot a gage would yield a higher value of pressure than its peers; on the next shot it might be the lowest. The difference in the pressure value extremes on a single shot averaged about 12 percent. The Sword Fish gages also showed great

scatter. In addition, many showed unexpected nonlinearity if the average value obtained from the standard gages was considered correct.

Because the changes in dynamic response of the Sword Fish gages were large compared to the changes in static KA that were measured, two shots in the series were fired in which gages were covered with unicellular foam rubber. The purpose was to eliminate the sharp shock front rise and replace it with a more gradual rise. If the suddenness of pressure rise were a factor in determining the gage dynamic response, then gages exposed to a gradual rise should yield more uniform results. Though a more gradual rise was attained and though there was some indication of improvement in the uniformity of pressure measurements, the improvement was neither consistent nor substantial.

After considerable study, it was realized that the standard gages were behaving as tourmaline piezoelectric gages had been for many years but that the Sword Fish gages were worse than usual and that some showed nonlinearity clearly for the first time.

The output of each gage relative to the average of the standard gages was plotted for each shock wave exposure as a function of the average pressure recorded by the standard gages. A series of one or more straight line segments was then drawn to represent the gage calibration. By linear extrapolation, these segments were extended from zero psi

to 10,000 psi, though the maximum pressure measured in the dynamic calibration was about 1,500 psi, and the minimum pressure was about 110 psi. Extrapolation in both directions was desired for convenience in machine computation.

The coordinate points of the straight line segments are given in Table 2.2 and constitute the dynamic calibration data for the Sword Fish tourmaline gages.

(U) 2.2.3 Lead Zirconate Hydrophones. On Station 4, at depths of 375 feet or more, lead zirconate hydrophones Transducer Type LC-10, Atlantic Research Corporation (ARC), Alexandria, Virginia, were used because tourmaline gages were of insufficient sensitivity to produce an acceptable signal level. Gages were vulcanized on lengths of cable furnished to the gage manufacturer, who also calibrated the gages (see Table 2.3). An ARC Type LC-32 hydrophone was used at Station 6.

After Sword Fish, four of the LC-10 hydrophones were dynamically calibrated with four of the same shots with which tourmaline gages were calibrated. The hydrophones were then recalibrated statically at pressures of 25, 50, 75, and 100 psi. All calibrations indicated that the hydrophones were nonlinear. Pronounced hysteresis was observable on some of the dynamic calibration records as failure of the record trace to return to hydrostatic pressure after passage of the shock wave. Dissection of these hydrophones showed cracked or shattered piezoelectric elements. Table 2.3 contains the

hydrophone calibration data.

2.2.4 Electrical Recording Equipment. Six of the seventeen Hardtack recorders were modified for use on Sword Fish; one of these served as a spare and was not used. The units are 10-channel magnetic tape recorders, with eight channels being used to record pressure data; the other two are used for a timing signal and a reference signal. The reference signal is used in playing back the records to reduce noise caused by tape speed variations.

The tape transport mechanisms, recording heads, and basic mechanical chassis of the Hardtack recorders were used with no changes. All other components of the recorders were redesigned and modified in various degrees in order to improve the reliability, efficiency, and convenience of operation of the recorders.

After returning from the field, it was realized that the two systems driving the recorder—the capstan drive and the tape take-up reel drive—contained gears which ran at slightly different speeds. The teeth in each caused a cyclical tape speed variation. The net tape speed variation was a result of the beating of the two gear trains. Though electrical compensation using the reference frequency was very effective, the remaining noise signal was, at best, about 3 percent of the full-scale data signals. For smaller signals, the proportion of noise to signal was proportionally greater. Since the Sword Fish pressure levels

were all lower than expected (because the ASROC missed the target), the gear noise had very serious effects on data analysis. Many of the techniques described elsewhere in this report were devised to minimize the interference of the gear noise with the data.

Changes were made in the modulators and cathode follower amplifiers for the piezoelectric gages to make the modulator frequencies less dependent on gage resistance and the main battery voltage used to power the equipment. These changes eliminated the problem of base frequency instability, which, during Hardtack, necessitated making frequent adjustments and caused the complete or partial loss of a number of channels of data. The modulators were further modified to reduce their power consumption.

One data channel each at Stations 1 and 2 was reserved for use by Project 3.1, "Studies of Shock Motion of Hull and Equipment". Also in support of the shock measurements at these stations, some simple mechanical accelerometers were used (see Appendix).

No frequency-modulated gage outputs of the Wiancko type, such as were used on Wigwam, were used.

As before, there were two time-base generators in each recorder. The former 2-Hz pulse generator was replaced by a 10-Hz electrically driven balance-wheel clock movement and pulse-shaping circuit. The output of this was superimposed upon one data channel; the square wave shape of these pulses

simplified separation of the data signal from them. The Hardtack scaler, which generated outputs of 10 kHz, 1 kHz, 100 Hz, and 10 Hz, was replaced by a 360-Hz self-powered, electrically driven tuning fork watch movement (Bulova Accutron) driving a pulse-shaping circuit. The frequency of this unit was accurate to one part in 15,000 (Table 2.4). The timing unit also incorporated a fiducial generator, which translated a fiducial pulse from a radio receiver into a shift in the base level of the 360-Hz pulse train, and also turned on the 10-Hz signal by means of a gate circuit. The fiducial generator served to prevent interference with the timing signal by spurious signals occurring after the fiducial pulse, and also simplified finding the location of the fiducial on the recorded tape.

The reference generator was the same as that used during Hardtack except that the frequency was reduced from 50 kHz to about 32 kHz (Table 2.4). The former frequency was unnecessarily high for compensation of tape-speed-variation frequencies that were present. Lowering the frequency also insured better recording of the reference frequency, which resulted in fewer dropouts on the tape. When used as a time-base, the reference frequency was calibrated with the Accutron output at the same part of the tape.

The dynamotor power supplies were replaced by transistorized dc-dc converters of greater reliability and efficiency.

The B+ regulator circuits were modified to maintain regulation at lower battery voltages and to increase reliability. The thermal delay relays used to allow filament warmup were replaced by more dependable transistorized delay circuits.

The batteries used to power the recorders were composed of new nickel-cadmium cells with the same capacity rating as those used during Hardtack, but with different dimensions requiring construction of longer battery cases. Two batteries instead of three were used in each recorder because of the better cell quality and approximately 35-percent reduction in power requirements. A new battery-charging circuit of increased convenience and efficiency was used.

The calibration multiple step generator was replaced by a calibration ramp generator of a new design. This new transistorized unit provided increased reliability, more uniform calibration signals, and greater accuracy by eliminating errors due to nonlinearities in the modulators and nonlinearities in the playback system.

The generator automatically applied a single calibration step and a single saw-tooth (ramp) voltage to the input of each data channel. The step was an ordinary "Q step" (Reference 9); however, the duration of the step was made of such length that capacitative coupling effects occurred in the input circuit and the input voltage dropped to a negative level when the step was terminated. After a very short pause,

the ramp was applied. Starting at the negative voltage following the termination of the step, the voltage was increased linearly with respect to time to a level above the highest expected signal and then was abruptly returned to zero (see Figure 2.6). Sufficient time was then allowed for the input circuit to recover before the data signal voltages were applied.

Use of the ramp is illustrated in Figure 2.6. Times are measured using the timing channel (or in mechanical analysis, the reference channel).

To determine a pressure, the following equations are used:

$$E_p = \frac{T_p - T_o}{T_s - T_o} E_c \qquad (2.4)$$

Where: E_p = data signal, volts

T_p = time at which projection of data deflection crosses ramp

T_o = time at which projection of base line crosses ramp

T_s = time at which projection of step deflection crosses ramp

E_c = calibration signal, measured, volts

and:

$$P = E_p \frac{C_s}{KA} \qquad (2.5)$$

Where: P = transient pressure in water, psi

C_s = standard capacitance, farads

KA = gage calibration, coulombs/psi

In actual use, the step base line and the data base line might not be identical; in this case, T_o for the data would be used in the numerator of Equation 2.4. Effects of system nonlinearity, assuming a linear gage output relative to pressure, are effectively eliminated by this method of calibration and record reading.

The sequence timer used during Hardtack was eliminated and its functions incorporated into the control unit. The control unit was simplified by using a minus-10-minute signal from the radio control to turn on the filaments and a signal at launch time to start the tape transport. Internal delay circuits were included to operate the bias supply and calibration generator. At about 100 seconds after launch, the control unit turned off all power and blew a fuse to prevent further operation. If the tests were cancelled at any time prior to the reception of the launch signal, the recorders would turn off and be ready for another cycle. After receipt of the launch signal, relays in the control units locked in, and the recorders could not be stopped. Delay of the launch signal for several minutes would not affect the operation of the recorders.

Minor rewiring of the recorder chassis and test units was done to accommodate the above changes.

2.2.5 The Playback System. The playback system (Reference 10) used on Sword Fish in the field was that which had been used on Hardtack. A minor modification was the repackaging of a transistor preamplifier and its relocation on the tape transport to minimize noise pickup.

After return from the field, the decision was made to modify the playback to permit simultaneous processing of all channels. The Sanborn Model 150 four-channel heated stylus recorder was replaced by two 7-channel dc amplifiers Model 1-162A, manufactured by Consolidated Electrodynamics Corporation, feeding a 24-channel string oscillograph, Minneapolis-Honeywell Visicorder Type 1612. The zero-signal dc output level at the data sampler output was set at zero using a potentiometer which replaced part of the output-stage-load resistor. Removal of sampler-generated transients and carrier frequency noise was accomplished by use of simple filter capacitors from the output to ground. Additional power supplies were required to operate all channels simultaneously. Permanent records of the galvanometer light traces were made on photo-sensitive paper and developed chemically. Deflections of several inches were obtained without loss of frequency response.

2.2.6 Electronic Pressure-Time Record Analysis. The use of a computer to calculate pressures, etc., from the Sword Fish records was necessitated by nonlinearities in the record-reproduce systems and in the gage calibrations. The paper

records produced by the Visicorder (Section 2.2.5) were measured using a Telereadex analog-to-decimal converter. Starting at a pressure wave arrival, readings were made at intervals of either 1 or 0.1 timing unit (approximately 0.0027776 second per unit). The value of displacement of the record trace from a reference trace at each point was punched on an IBM card. The calibration ramp and step were similarly measured. Separate cards containing gage dynamic calibration data (Section 2.2.2), calibration capacitances, step voltages, and time increments were punched.

A program was written by W.H. Faux, Naval Ordnance Laboratory (NOL), for the IBM 7090 computer to convert the measurement on the cards to the desired physical values. In the computer, each pressure reading was compared with ramp readings, and the voltage necessary to achieve the reading was computed. Starting with the KA value for the particular gage at 10,000-psi pressure, and using calibration capacitance and the computed voltage, the pressure was calculated. By successive approximations, the calculated pressure and the pressure at which the gage calibration was selected were brought reasonably close together. This pressure value was one output of the machine; it also calculated the $\log_{10}$ of the pressure, the incremental impulse, and the incremental energy. The latter two items were added to preceeding totals so that the five primary printed outputs were pressure, $\log_{10}$ pressure, total impulse, total energy,

and time. Impulse, energy, and time were given as the total to the measured point from the first reading. Shock wave pressure and $\log_{10}$ pressure as a function of time were mechanically plotted to aid in the determination of the shock wave time constant.

(U) 2.2.7 Mechanized Data Analysis. After the work described in the previous section had been completed, another method of machine analysis became available which more fully and more directly used the information on the original tape records.

The reference frequency that was recorded at shot time was calibrated against the 360-Hz time base recorded at shot time. The voltage output from a data channel at playback time was sampled at the reference frequency and each sample digitized and recorded in digital format on a new tape. Step, ramp, and pressure record were all digitized.

The digitized data were used as input to a computer program that smoothed the data where necessary; established base lines; detected the presence of the three functions: step, ramp, and shock (or other desired pressure pulse); and finally, using the essential parts of the Faux program, computed time, pressure, log of pressure, impulse, and energy and printed them in table form.

The pressure output values from the digitizing program were also recorded on magnetic tape. This tape then supplied input to a data reduction program. The data reduction program:

1. Calculated the time constant by progressively making a least square fit to regenerated log of pressure versus time data at increasing times.

2. Calculated the extrapolated peak pressure assuming that the recorder rise time prevented the true peak pressure from being observed. The extrapolation was based on the best fit line obtained in "1" above.

3. Noted the time at which the elapsed time and the current time constant were equal.

4. Reported the values of impulse and energy at that time.

5. Computed and tabulated reduced pressure and reduced time values where the standards were the extrapolated peak pressure and one time constant.

6. Prepared instructions for mechanical plotting and recorded them on magnetic tape.

The mechanical plotter could make plots of pressure, log of pressure, impulse, energy, and reduced pressure versus time. It could also make a plot of reduced pressure versus reduced time.

The principle virtues of the mechanized-data-reduction were that the sampling rate was about 80 times that of the manual data reduction, and the effect of gear and other noise on the analysis was greatly reduced. Rather than guessing or estimating which part of the data should be used, all of the data was used.

Considerable flexibility was built into the system so that the analyst had various input options (tape or cards), choice of sampling rate, opportunity to override the calculated time constant or calculated peak pressure, degree of smoothing, and choice of plots, or none. Print out from only the digitizing program was available without running the data reduction program.

Figure 2.7 and Table 2.5 are given to permit comparison of results obtained by manual and mechanical reading of the Sword Fish data.

2.2.8 Mechanical Support and Rigging. The same general types of gage placement, gage suspension, and recording instrument protection that were used during Hardtack were used for Sword Fish. Changes were made to expedite gage setting, minimize water drag on the cable bundles, simplify servicing of the electronic gear, and protect instrumentation against specific hazards noted during Hardtack.

When Willow was first proposed, the glass-foam-filled lower compartments of all the Hardtack instrument containers were cut off so that the containers could be used below decks on YC barges. The remaining instrument chambers, although less buoyant, would float.

Experience during Operation Hardtack showed that a two-directional shock-absorber system was necessary at close-in stations to prevent damaging rebound of the instrument container. The Hardtack instrument protection system used two

absorber elements to reduce any upward shock to not more than 5 gravities acceleration at the container. For Stations 1 and 2 (close-in) on Sword Fish, the same system was used, but one of the elements was inverted (see Figure 2.8) to protect against downward shock. Though only one absorber for upward shock remained, the maximum expected acceleration at the instrument container was about 3.75 gravities because the container weights were reduced from 600 pounds (Hardtack) to 450 pounds (Sword Fish). If the weight had not been reduced, the maximum acceleration would have been only 2.5 gravities. The allowable cone travel due to shock loading was reduced from 5 to 2 feet because less than 8 inches of travel was used under the most severe conditions on Hardtack.

On three ship stations, the instrument containers were placed on thick foam rubber and held down by three shock cords or manila rope. The electrical cable entry into the container was bolted on without any quick release mechanism, since no ship was expected to sink.

As during Hardtack, the multi-gage strings were supported on 1/2-inch non-twist wire rope. At Stations 1, 2, and 3, electrically driven winches previously used on Hardtack were used to lower the cables. At Stations 1 and 2, winch power was supplied by gasoline-engine-driven generators; at Station 3, by the ship's auxiliary plant. At Station 4, a ship's winch that had adequate cable capacity was used. At Station 5, the gage string was short enough to be preassembled and

set as follows: The string and its sinker were lashed horizontally to the side of the ship. The head of the string was secured, and the sinker was lowered by the ship's winch using a 3/8-inch wire-rope cable. When the gage string reached a vertical altitude and supported the sinker, the lowering cable was slacked off, transferred forward, and secured so that it towed the sinker while the ship was under way. At Station 6, the single hydrophone was lowered by hand.

On Stations 1, 2, and 3, all EPT and BC gages were jointly supported by single wire ropes. No safety cable was provided for saving the BC gages if the 1/2-inch wire rope broke. Brackets for attaching both PE and BC gages were similar to those used on Hardtack; however, new types of frames were used for attaching the PE gages and cables to the BC blocks (see Figure 2.9). The new bracket permitted use of the BC gage block cable clip to support the PE brackets. To minimize snagging during handling, and water drag when set, the electrical cable bundles were sheathed with solvent-sealed, zipper-type, vinyl jacketing.

Because the cables were expected to be supported overboard for only about 24 hours, outboard suspension of the cables as was used on Hardtack was replaced by suspension from steel chain directly alongside the ship or barge. Special attachments were made for fastening the 1/2-inch wire rope to the chain so that, when fully lowered, only the chain

would be under load where chafing could occur. The electrical cable bundle and loose steel cable were led fore and aft along the side of the vessel so that they could not be pinched or rubbed by the chain. At Stations 1 and 2, the bitter ends of the steel cable were taken off the winch and rigged as a safety line in case the chain should break and, also, for possible transfer to an LCM for recovery purposes.

Location of the gage strings on the starboard side of the platforms and ships on which they were suspended was as follows: (1) Stations 1 and 2, 12 feet from stern; (2) Stations 3 and 5, ship's Frame 135; (3) Station 4, ship's Frame 63; and (4) Station 6, cobbler's shop.

2.3 PRESHOT OPERATIONS

The experimental arrangements were worked out in January 1962 for a May firing date. Work then proceeded at NOL on revisions of the Hardtack recorder design and detailed planning of the various stations. In February, orders were placed for long-lead-time supplies. Preparation of gages was commenced by an NOL group at the Naval Ordnance Station, Indian Head, Maryland. This group also prepared the winces and commenced refurbishing the Hardtack recorders. Shop work was done at NOL preparing instrument supports, cable connectors, and other hardware.

On 14 March, the first shipment (winces, hardware, generators, and ball crusher gages) was dispatched to San Diego. On 22 March, cable for hydrophone installation was sent to Atlantic Research Corporation, Alexandria, Virginia.

On 30 March, the second shipment (electronic recorders and hardware) was sent to San Diego.

Beginning on 5 April, project personnel in small groups reported at the Naval Repair Facility, San Diego, California, for field work. At Indian Head, work on the piezoelectric gages and cable bundling was completed on 8 April. On 13 April, the final shipment, which included the Hardtack playback system, was sent to San Diego. On 24 April, the last project personnel reported; and on 28 April, the project was ready for participation in the sea trials.

During the sea trials, each station was manned by the personnel to be assigned for the shot. All functions were performed, except that very few gages were actually lowered into the water because the hazards of setting and recovery were too great to risk with the irreplaceable gages and cables. Upon completion of sea trials, equipment was readied for the actual operation. Two project personnel were assigned to each station and went to sea on the ship carrying that station. In addition, four to six ship's personnel were assigned to help in the setting of each station. All electronic recorders were loaded with tape, batteries were charged, and all internal adjustments made before departure.

2.4 SHOT OPERATIONS

Final preparations were made on 9 May 1962, and all equipment was ready for a shot on 10 May. Most project

operations proceeded on schedule, though some delay occurred at Station 1.

The short delay, which was caused by difficulty in making up the array, did not affect the scheduled shot time. After the countdown passed the minus-10-minute time, a series of holds occurred which expended a total of about 18 minutes of running time from the recorder batteries. Though restarting the cycle at minus 10 minutes would have been possible, the reliability of the equipment was seriously impaired. It was also thought that the zero (launch) time signal had been sent, which would have run the tape transports; therefore, the project advised postponement of the shot.

A number of courses of action were possible, but the decision was made to recover all gear. During this operation, the electrical cables at Station 4 were cut by the ship's propeller, but all gages were recovered. The cables were subsequently spliced. Upon reentry, it was discovered that improper rigging had dropped the instrument container at Station 2 to the deck. Superficial checks and repairs were made and the unit returned to service. A spare recorder could not be made ready by the next day, and complete testing of the damaged unit at sea was not possible. When the BC gages were examined, it was noted that many appeared to have leaked. This was attributed to permanent set of the O-ring seals under the rubber waterproofing membrane. The set was caused by the long period (about 60 days) between gage

assembly and use. Some gages were dried and reloaded, others were drained and resealed, but most were merely tightened as they were being set the next day.

On 11 May the operation was repeated, starting 1 hour later in the morning but with the same scheduled shot time. Since the towline was assembled more expeditiously, the project was ready ahead of schedule, and the shot went as planned.

During the recovery operations, the towed array was left slack for a while and later towed on a course to starboard, somewhat across the wind. This caused the USS BAUSELL and the platforms to ride against the vertical gage strings, preventing recovery at the USS BAUSELL for at least 6 hours. At about 2-1/2 hours after shot time, the platforms were washed down and recovery accomplished in about 2 hours, despite the unfavorable towing course. Most damage to the gages and cables was caused by rubbing on the sharp bottom corners of the platforms.

Because of severe twisting, the lower section of the electrical cables at Station 1 had to be cut to permit recovery. After the platform stations were secure, the tow was detached from the USS BAUSELL and the string there recovered at about 2000 hours. Project personnel, though their work was completed by 1730 on 11 May, were either in LCM boats or on the platforms from about 1330 on 11 May until 0040 on 12 May.

2.5 POSTSHOT OPERATIONS

The Hardtack playback equipment was activated and all tapes played back with various paper speeds to obtain an overall picture of what results were obtained and also what phenomena were significant at the various stations. The BC gages were opened and the balls measured. All equipment in usable condition (or reparable) that would not be required for report writing was packed and sent to NOL. The field work was completed, and the draft report submitted on 2 June 1962.

Upon return to the Naval Ordnance Laboratory, the Hardtack playback system was modified to permit simultaneous playback of all data and timing channels through a string galvanometer recorder. All EPT records were replayed and remeasured for electronic computer data reduction. New calibrations were obtained for both BC and EPT gages. The sound velocity-depth profile data was used with refraction theory to correct the pressure measurements to free field values. The final report was completed.

2.6 COMPUTATION OF SHOCK ARRIVAL TIMES

Application of the shock wave ranging method of determining the depth of burst of Shot Sword Fish was made difficult by shock wave-velocity changes in the ocean water at the test site and the uncertainty of the burst location relative to the gage liner. Refraction computational codes

used in studying sound propagation in the sea do not include corrections for finite-amplitude waves and are not conveniently arranged for determining arrival times at specific points in space. To make the computations for Sword Fish, a simplified computing program was set up that used straight-line propagation and corrected for high-amplitude shock and the local sound velocity as determined from the sound-velocity profile. The change in ray path length due to ray curvature for Sword Fish through distances from 0 to 3,000 feet was found to be negligible by comparing a straight path and a curved ray path computed using a code that did include refraction. The program is described here because it was a tool, part of the procedure for making the test, and was not dependent on data acquisition for its development.

Computation of shock arrival times: A plot of pressure versus shock velocity was made using data from Reference 11. An empirical equation was derived expressing the shock velocity as a function of pressure:

$$U = c(z) + aP + bP^2 \qquad (2.6)$$

Where: U = shock velocity, ft/sec

$c(z)$ = velocity of sound expressed as a function of depth, ft/sec

P = shock wave pressure, psi

$a = 2.902 \times 10^{-2}$, ft-in^2/lb-sec

$b = 1.299 \times 10^{-7}$, ft^2-in^4/lb^2-sec^2

The equation used for expressing pressure at any point along a path as a function of the distance from the charge is (Reference 12):

$$P = 4.38 \times 10^6 \, (Y^{1/3}/R)^{1.13} \qquad (2.7)$$

Where: Y = yield, kt

R = slant range, feet

The equation used for expressing the depth as a function of the distance along the path from the charge to the gage position is:

$$z = z_o - \frac{R\,(z_o - G)}{\sqrt{H^2 + (z_o - G)^2}} \qquad (2.8)$$

Where: z = depth at which shock velocity is being evaluated, feet

z_o = depth of burst, feet

G = depth of gage, feet

H = horizontal range from charge to gage string, feet

After substituting Equation 2.7 for P in Equation 2.6, and dividing both sides of Equation 2.6 by $Y^{1/3}$, the reduced shock velocity is:

$$U_{\ell} = \frac{1}{Y^{1/3}} \left[c(z) + a' \left(\frac{1}{L}\right)^{1.13} + b' \left(\frac{1}{L}\right)^{2.26} \right] \qquad (2.9)$$

Where: $L = R/Y^{1/3}$, ft/kt$^{1/3}$

$U_L = dL/dt$, ft/kt$^{1/3}$/sec

$a' = a(4.38 \times 10^6)$

$b' = b(4.38 \times 10^6)^2$

In order to get the shock front arrival time, T, Equation 2.9 must be integrated:

$$T = Y^{1/3} \int_{L_o}^{L} \frac{dL}{c(z) + a'\left(\frac{1}{L}\right)^{1.13} + b'\left(\frac{1}{L}\right)^{2.26}} + T_o \quad (2.10)$$

where T_o and L_o must be determined. The method used to determine L_o and T_o is as follows:

$$P_1 = K\,(Y_1^{1/3}/R_1)^{1.13}$$

$$P_2 = K\,(Y_2^{1/3}/R_2)^{1.13}$$

$$\frac{P_1}{P_2} = \left(\frac{Y_1^{1/3} \times R_2}{Y_2^{1/3} \times R_1}\right)^{1.13}$$

The boundary conditions used are $P_1 = P_2$, when P_1 equals 25,000 psi, and Y_1 equals 31 kt (Wigwam conditions), therefore:

$$L_o = 96.49 \text{ ft/kt}^{1/3}.$$

The value for T_o for any yield, Y, was found in a similar manner and is expressed as:

$$T_o = 0.0112\ Y^{1/3} \text{ sec}$$

The value of 25,000 psi for the pressure limit was used, because Equation 2.7 is not considered reliable for higher pressures.

Equation 2.10 was programmed, using a Gaussian Quadrature, and tested by using the Wigwam profile and comparing computed arrival times with measured values at a range of 11,000 feet. Differences of less than 1.0 msec between the two values were obtained, and this accuracy was judged adequate for the intended use.

TABLE 2.1 INSTRUMENTATION DATA FOR EACH INSTRUMENTED POINT.

For location of stations, see Figures 2.1 and 2.2.

Station Number	Depth	Type of Gage	Gage Number	Gage Element Size	Tape Recorder Number	Channel[a]
	feet			inches		
1	25 to 1,000 every 25 feet	BC[b]		3/8		
	50	PE[c,d]	1,868	1/2	7	1
	375		1,940	7/8	7	7
	700		1,634	1-1/8	7	2
	1,025		1,638	1-1/8[e]	7	8
	1,350		1,639	1-1/8[e]	7	3
	1,675		1,401	2	7	9
	1,995		1,403	2	7	4
			360.02 Hz		7	6
2	50 to 1,000 every 50 feet	BC		3/8		
	25 to 975 every 50 feet	BC		5/32		
2	50	PE	1,865	1/2	12	1
	375		1,635	1-1/8	12	7
	700		1,630	1-1/8	12	2
	1,025		1,657	1-1/8[e]	12	8
	1,350		1,640	1-1/8[e]	12	3
	1,675		1,407	2	12	9
	1,995		1,400	2	12	4
			360.02 Hz		12	6

TABLE 2.1 (Continued)

Station Number	Depth	Type of Gage	Gage Number	Gage Element Size	Tape Recorder Number	Channel[a]
	feet			inches		
3	25 to 1,000 every 25 feet	BC		5/32		
	25	PE	1,941	7/8	17	1
	50		1,456	7/8	17	7
	375		1,658	1-1/8[e]	17	2
	700		1,582	2	17	8
	1,025		1,586	2	17	3
	1,350		1,585	2	17	9
	1,675		1,644	2	17	4
	2,000		1,584	2	17	10
			360.04 Hz		17	6
4	25	PE	1,583	2	5	1
	50		1,646	2	5	7
	375	PEH[f]	4C	LC-10	5	2
	700		4D	LC-10	5	8
	982		4E	LC-10	5	3
	1,307		4F	LC-10	5	9
	1,632		4G	LC-10	5	4
	1,957		4H	LC-10	5	10
			360.04 Hz		5	6
5	20	PE	1,575	1-1/8[e]	9	1
	30		1,576	1-1/8[e]	9	7
	40		1,404	2	9	8
	50		1,405	2	9	2
			360.04 Hz		9	6
6	200	PEH		LC-32	Sony	1
			360 Hz			2

[a] Channel 5 of each recorder was the reference channel.
[b] Three ball crusher gages mounted in each block. Fourth mounting hole used with PE bracket.
[c] Tourmaline piezoelectric gage.
[d] Four-pile gage unless otherwise noted.
[e] Eight-pile gage.
[f] Lead zirconate-titanate piezoelectric hydrophone (gage).

TABLE 2.2 CALIBRATION DATA FOR TOURMALINE GAGES.

Station	Depth	Gage	Diameter of Plates	Number of Plates	Static KA, μμcoulombs/psi				Dynamic KA, μμcoulombs/psi, Smoothed for Use in Computations							
					Manufacturers' Calibration[a]	Naval Ordnance Laboratory Calibrations			Pressure Level, psi							
						Fall 1961[a]	November December 1962	March April 1963	0	250	400	600	900	1,200	1,500	10,000
	feet	number	inches													
1	50	1,868	1/2	4	7.79	7.99	Not on cable	7.67	4.22	--	--	5.00	--	--	7.06	7.67
	375	1,940	7/8	4	23.6	24.0	Not on cable	23.8	14.	--	--	16.4	--	--	25.	25.
	700	1,634	1-1/8	4	39.3	39.7	39.8	39.5	32.	--	--	--	--	--	41.1	41.1
	1,025	1,638	1-1/8	8	84.4	84.5	83.5	85.8	40.3	52.3	59.2	69.1	79.8	85.8	91.8	91.8
	1,350	1,639	1-1/8	8	85.1	84.7	82.0	85.6	79.6	--	--	--	--	--	88.2	88.2
	1,675	1,401	2	4	128.2	131.	128.7	--	109.4	--	--	--	--	--	146.7	146.7
	1,995	1,403	2	4	164.8	137.	135.8	--	112.7	--	--	--	--	--	149.4	149.4
2	50	1,865	1/2	4	7.84	8.05	8.09	8.11	2.43	--	--	5.07	--	--	9.73	10.0
	375	1,635	1-1/8	4	44.0	41.3	Shorted	Shorted	35.6	--	--	--	--	--	45.8	45.8
	700	1,630	1-1/8	4	39.0	39.6	39.7	39.9	33.9	33.9	34.4	35.1	37.5	43.1	49.4	49.4
	1,025	1,657	1-1/8	8	81.2	81.2	Shorted	79.5[a]	67.6	--	--	--	--	--	78.7	78.7
	1,350	1,640	1-1/8	8	81.6	82.4	83.0	--	83.0	--	--	--	--	--	91.3	91.3
	1,675	1,407	2	4	212.	150.2	141.1	--	134.	--	--	--	--	--	172.	172.
	1,995	1,400	2	4	162.5	129.5	Open	129.1	129.1	--	--	--	--	--	--	129.1
3	25	1,941	7/8	4	23.7	24.0	24.0	24.4	14.3	--	--	16.8	--	--	25.6	25.6
	50	1,456	7/8	4	24.9	25.7	26.1	26.4	17.2	--	--	--	--	--	32.5	32.5
	375	1,658	1-1/8	8	83.7	86.7	Shorted	84.6[a]	71.5	--	--	--	--	--	83.8	83.8
	700	1,582	2	4	127.6	126.	125.1	128.1	105.	--	--	--	--	--	150.	150.
	1,025	1,586	2	4	126.4	125.2	126.2	--	107.	--	--	--	--	--	145.	145.
	1,350	1,585	2	4	122.8	125.5	126.	125.1[a]	126.	--	--	--	--	--	155.	155.
	1,675	1,644	2	4	123.9	125.1	126.	--	101.	--	--	--	--	--	135.	135.
	2,000	1,584	2	4	130.6	131.3	130.2	--	108.	--	--	--	--	--	143.	143.
4	25	1,583	2	4	123.9	124.5	126.2	128.8	116.	--	--	--	--	--	151.	151.
	50	1,646	2	4	122.	123.3	Low resistance	123.3	99.	--	--	--	--	--	132.	132.
5	20	1,575	1-1/8	8	82.8	84.2	83.2	86.4	68.3	75.6	80.2	86.4	93.3	97.6	102.	102.
	30	1,576	1-1/8	8	74.6	81.4	81.7	--	64.5[b]	--	--	81.7	88.2	--	96.4	96.4
	40	1,404	2	4	126.	133.	130.7	Shorted	136.	--	--	144.	--	--	158.	158.
	50	1,405	2	4	130.	132.9	134.7	132.9[a]	135.	--	--	--	--	--	159.	159.

[a] Bare gage, not waterproofed.
[b] Dynamic calibrations were derived for this gage after the electrical conductor to one plate was broken. This was not discovered until computations were completed.

TABLE 2.3 HYDROPHONE CALIBRATIONS AT STATION 4.

Type LC-10 M1 positive polarity output. The known temporal sequence of calibrations is tabulated downward for each hydrophone.

Depth	Hydrophone Number	Calibration, KA μμcoulombs/psi, At Noted Pressures								
		Pre-Shot			Post-Shot					
		Manufacturers' Static			NOL Dynamic		NOL Static			
		25 psi	50 psi	100 psi	339 psi	120 psi	25 psi	50 psi	75 psi	100 psi
feet										
375	4C	761	776	795		716 685	544	583	596	648
700	4D	625	630	666	892	653 614	509	550	578	620
982	4E	627	642	683	555[a]	663 608	507	570	622	653
1,307	4F	788	810	873	Shorted	--	--	--	--	--
1,632	4G	548	558	597	Shorted	--	--	--	--	--
1,957	4H	536	546	588	784	Open	--	--	--	--

[a] No error discovered in record reading, but this value is not consistent with data from other hydrophones. The wrong calibration step voltage may have been recorded.

TABLE 2.4 TIME BASE DATA.

Station	Recorder	Timing Frequency	Sampling Region	Reference Frequency
		Hz		Hz
1	7	360.02	At shock wave	32,527 ± 54
2	12	360.02	At shock wave	32,488 ± 32
3	17	360.04	At shock wave	33,124 ± 90
4	5	360.04	At calibration step	33,048 ± 58
			At shock wave	33,037 ± 75
			At bottom reflection	33,034 ± 55
5	9	360.04	At calibration step	32,393 ± 49
			At shock wave	32,389 ± 49

TABLE 2.5 COMPARISON OF DATA REDUCTION SYSTEMS.

Recorder 7, Channel 8	Fixed Calibration	
	Manual Reading	Mechanical
Sampling frequency	360/sec	32,526/sec
Number of data points at 1 θ	11	883
Peak pressure, psi	1,261	1,277.7
Time constant, θ, seconds	0.0270	0.02627
Impulse (total), psi-sec (to 1 θ)	33.8 22.9	33.4 21.2
Energy (total), in-lb/in^2 (to 1 θ)	4,184 3,546	4,160.9 3,511
Gage KA, μμcoulombs/psi	87.02	87.02

Also see Table 4.5.

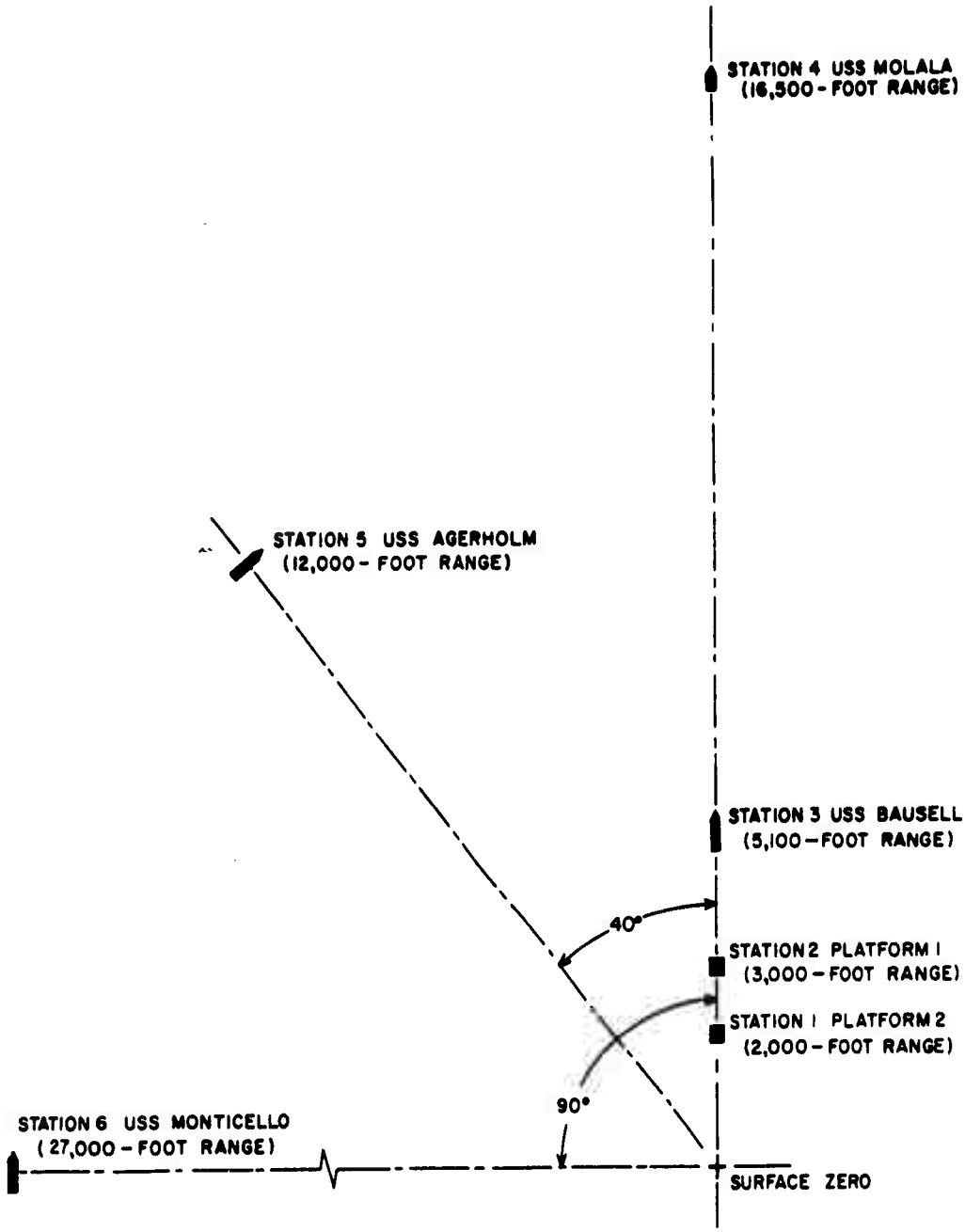

Figure 2.1 Planned locations of pressure-measuring stations.

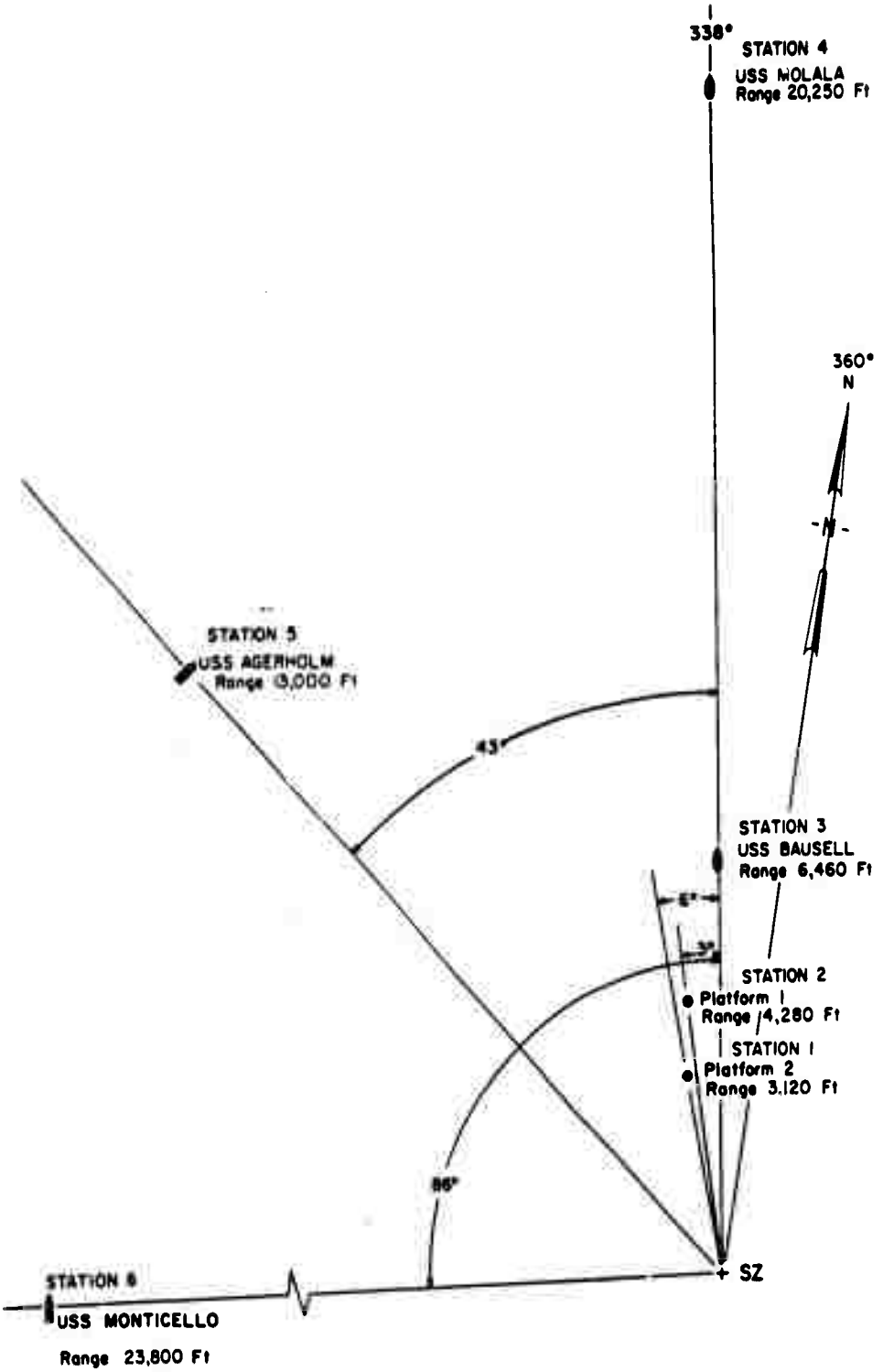

Figure 2.2 Actual deduced locations of pressure-measuring stations.

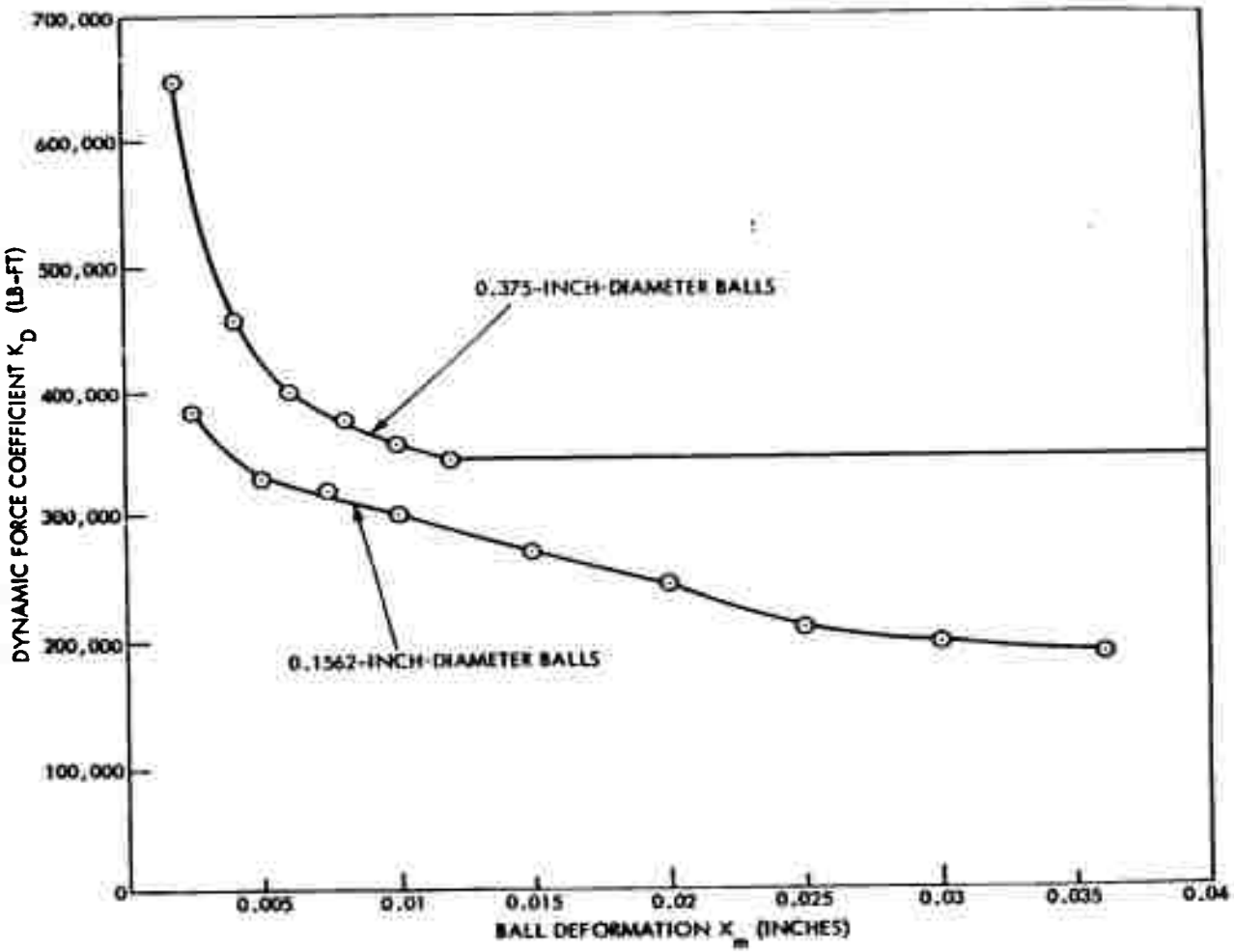

Figure 2.3 Dynamic force coefficients, copper balls.

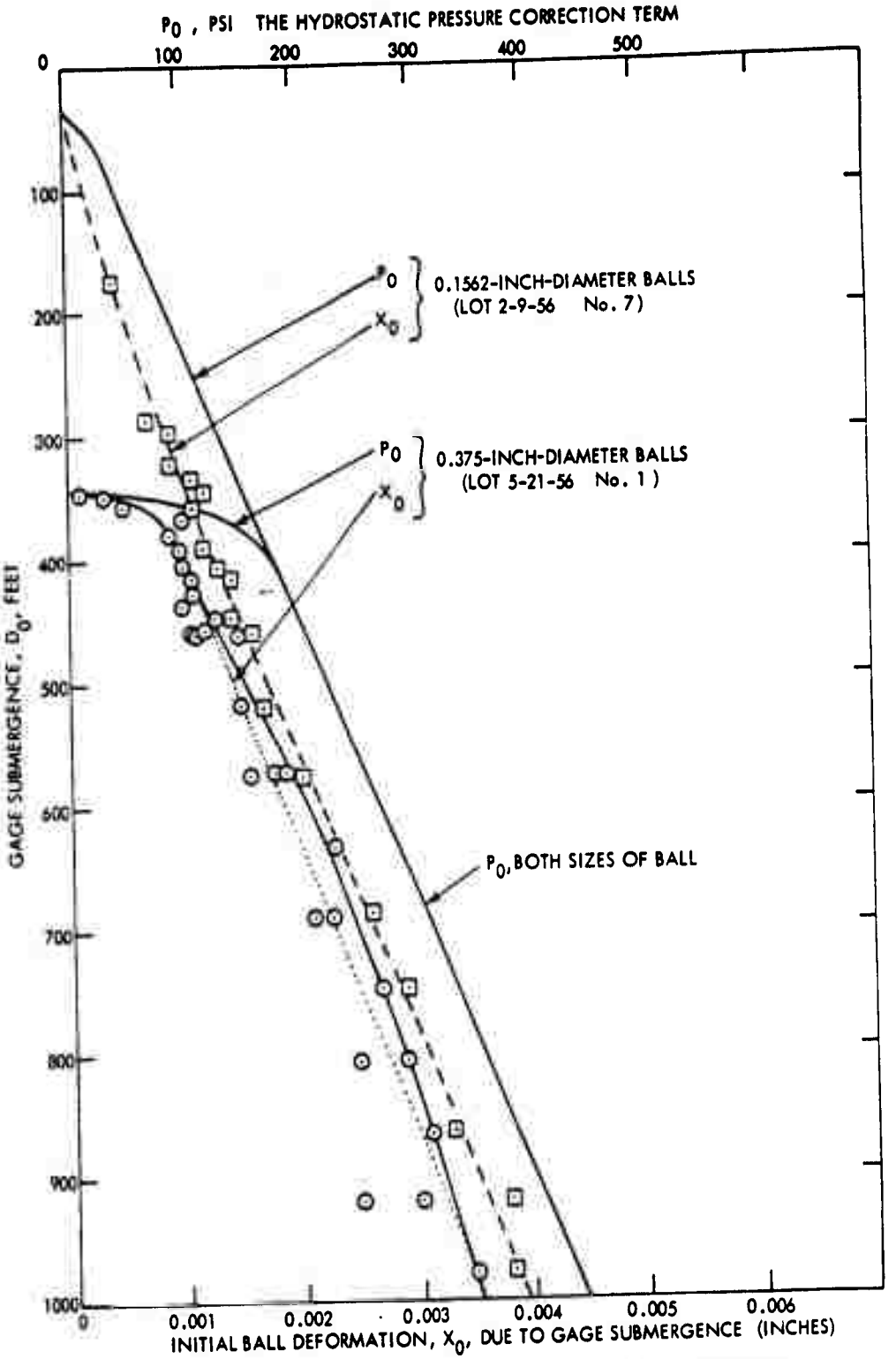

Figure 2.4 Initial ball deformation and the hydrostatic pressure correction term, copper balls.

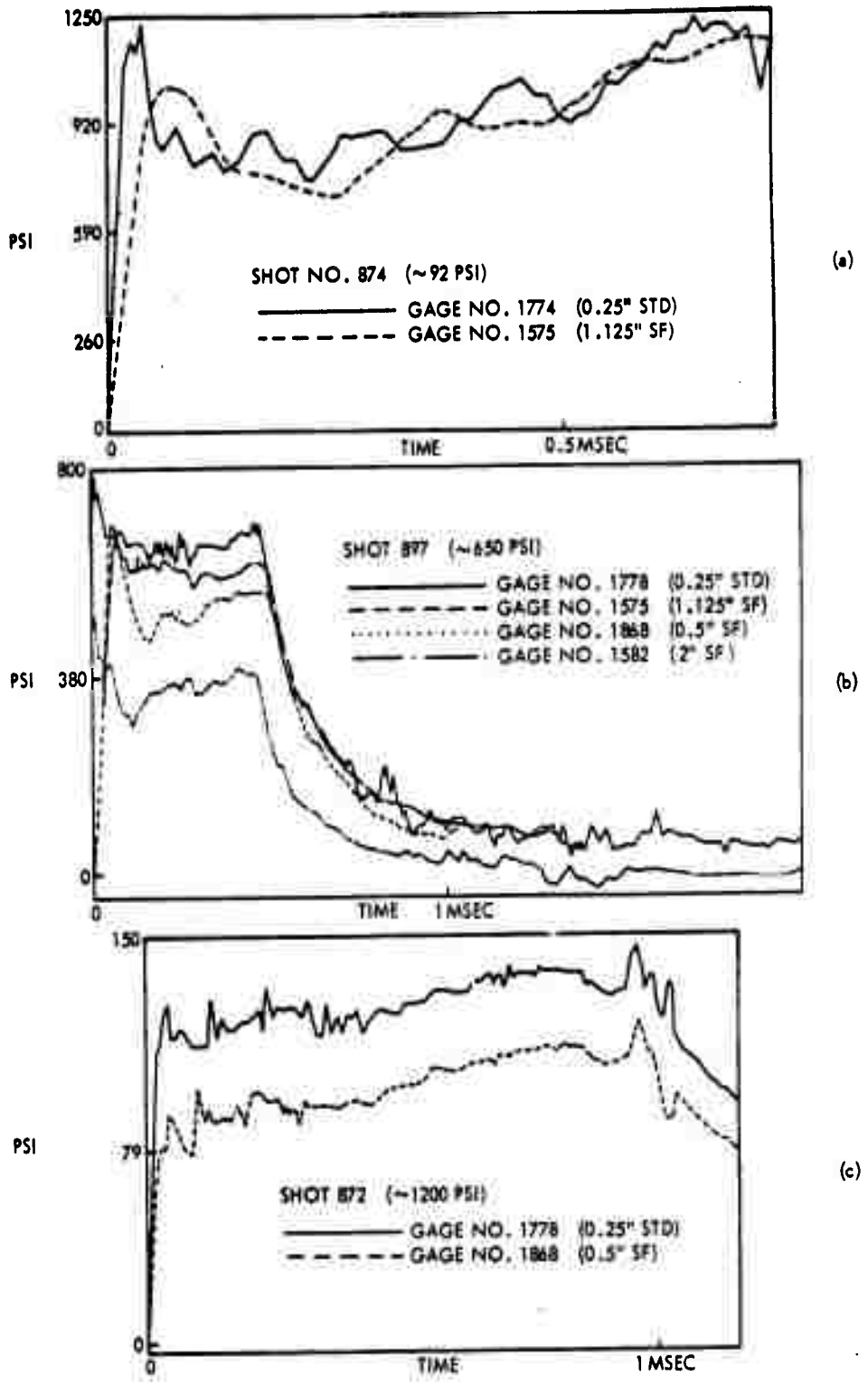

Figure 2.5 Dynamic calibration shock waves.

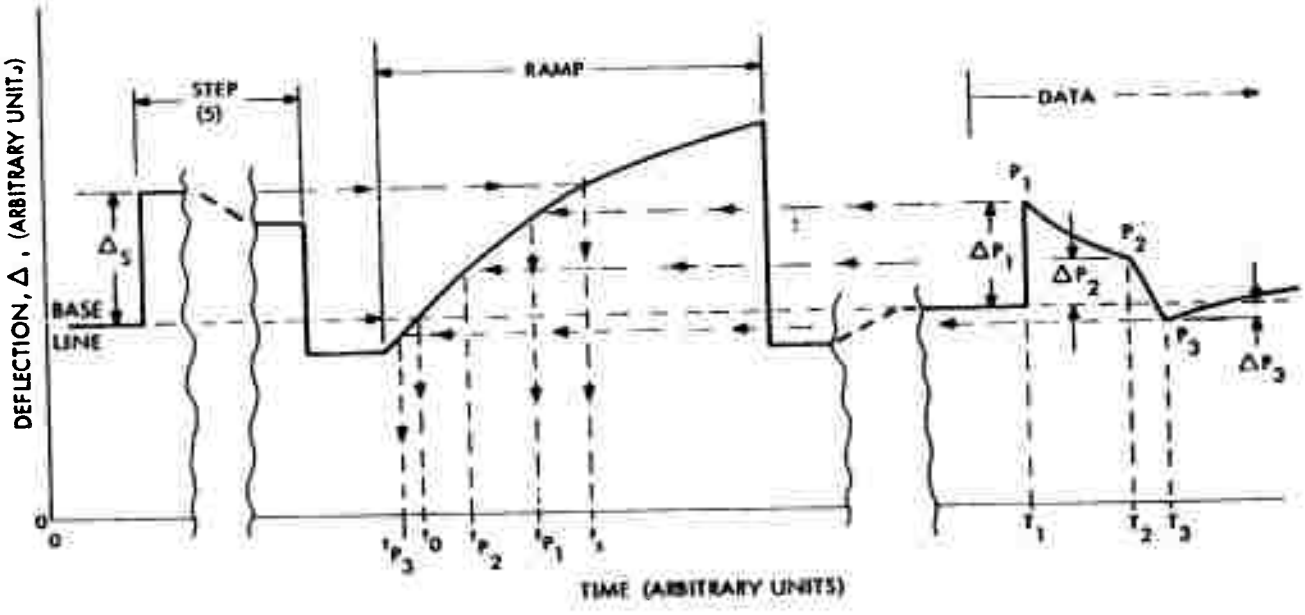

T = TIME OF EVENTS

t = TIME AT WHICH PROJECTIONS FROM VARIOUS EVENTS CROSS RAMP

Δ = DEFLECTION OF TRACE ON PLAYBACK RECORD

P = TYPICAL PRESSURE EVENTS

NOTE THAT THE RAMP WAS A LINEARLY INCREASING VOLTAGE AND THAT THE OBSERVED CURVATURE IS DUE TO SYSTEM NON-LINEARITIES.

Figure 2.6 Schematic of calibration and data signals during playback.

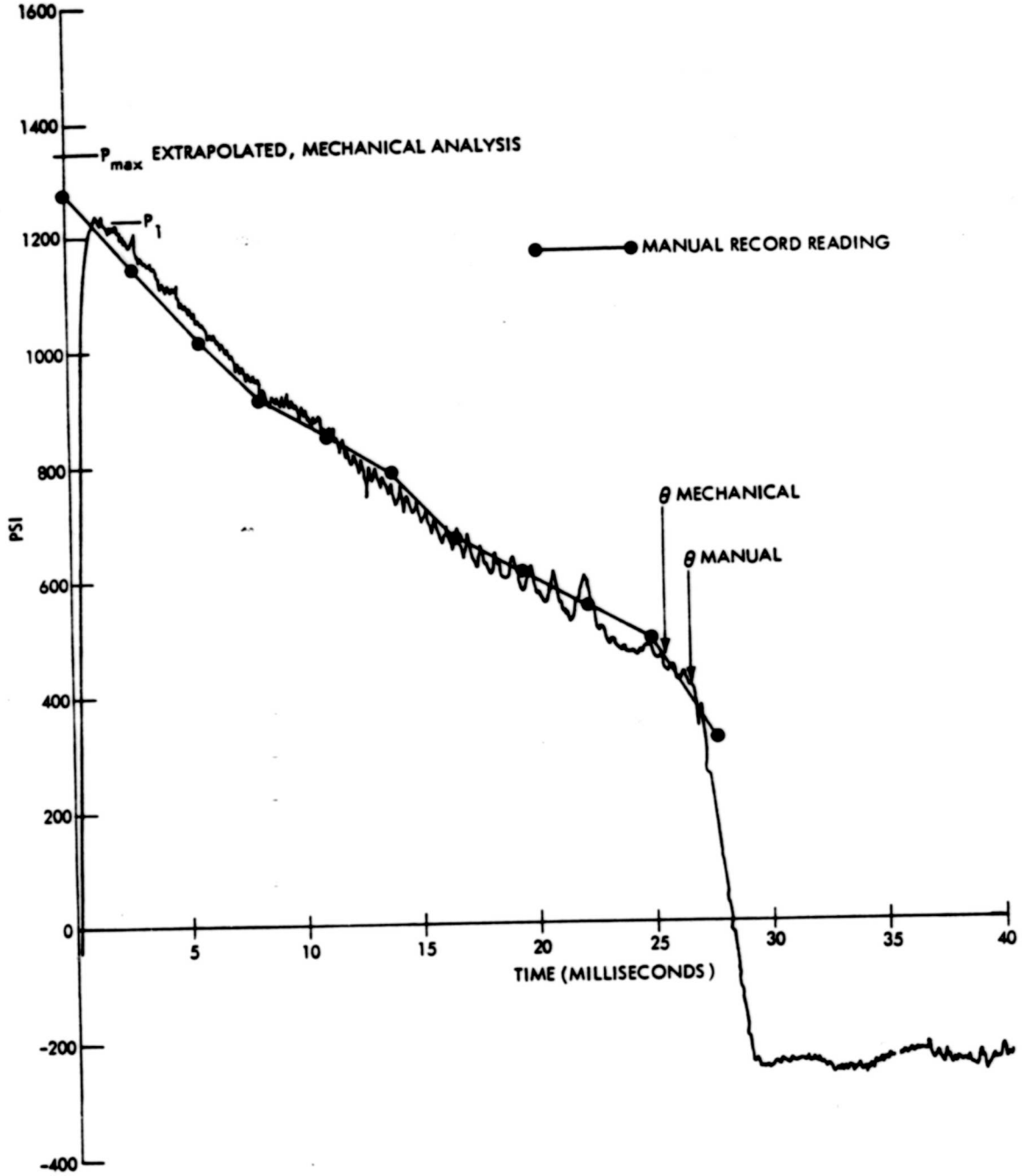

Figure 2.7 Comparison of manual and mechanical record reading.

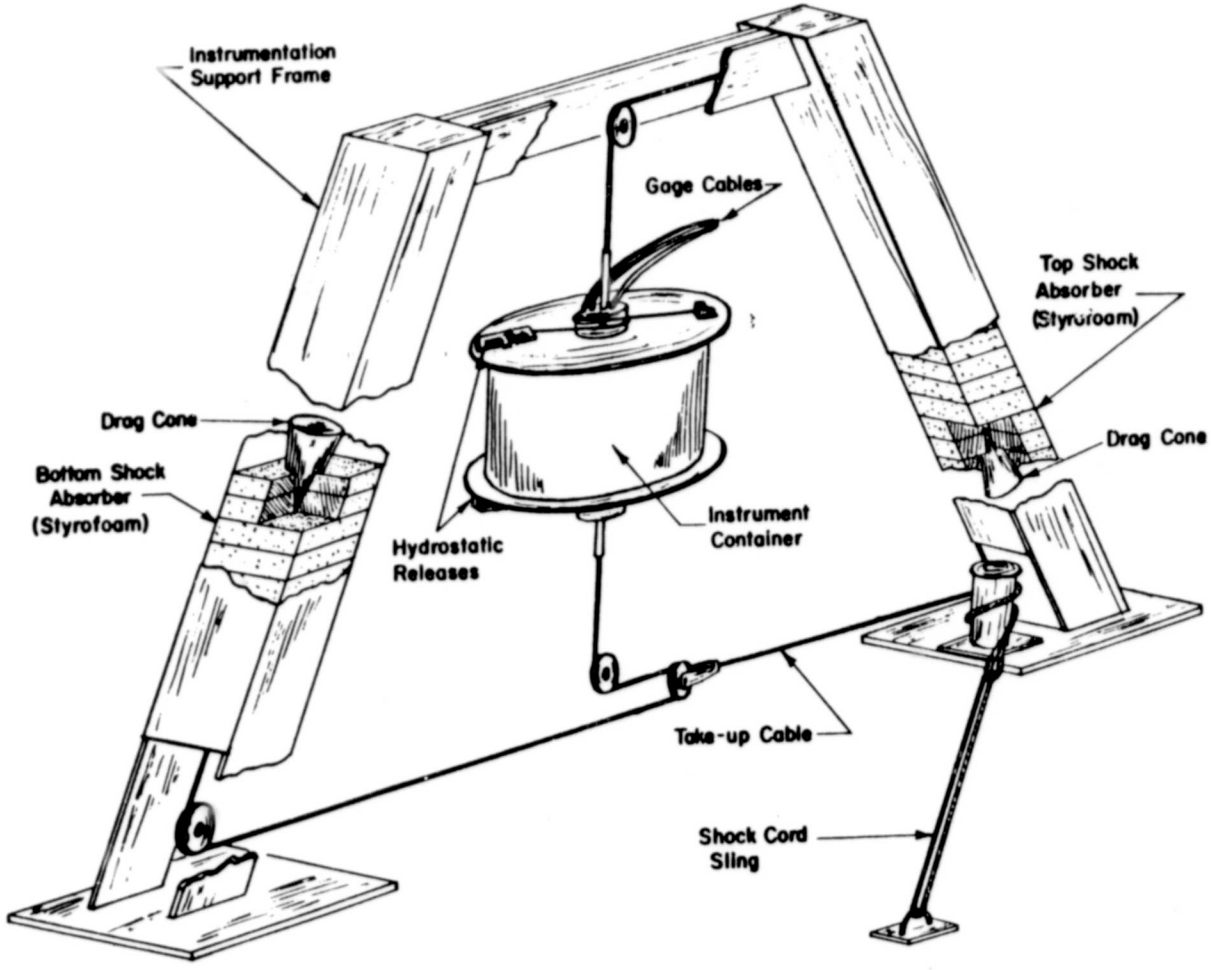

Figure 2.8 Instrument container at Stations 1 and 2.

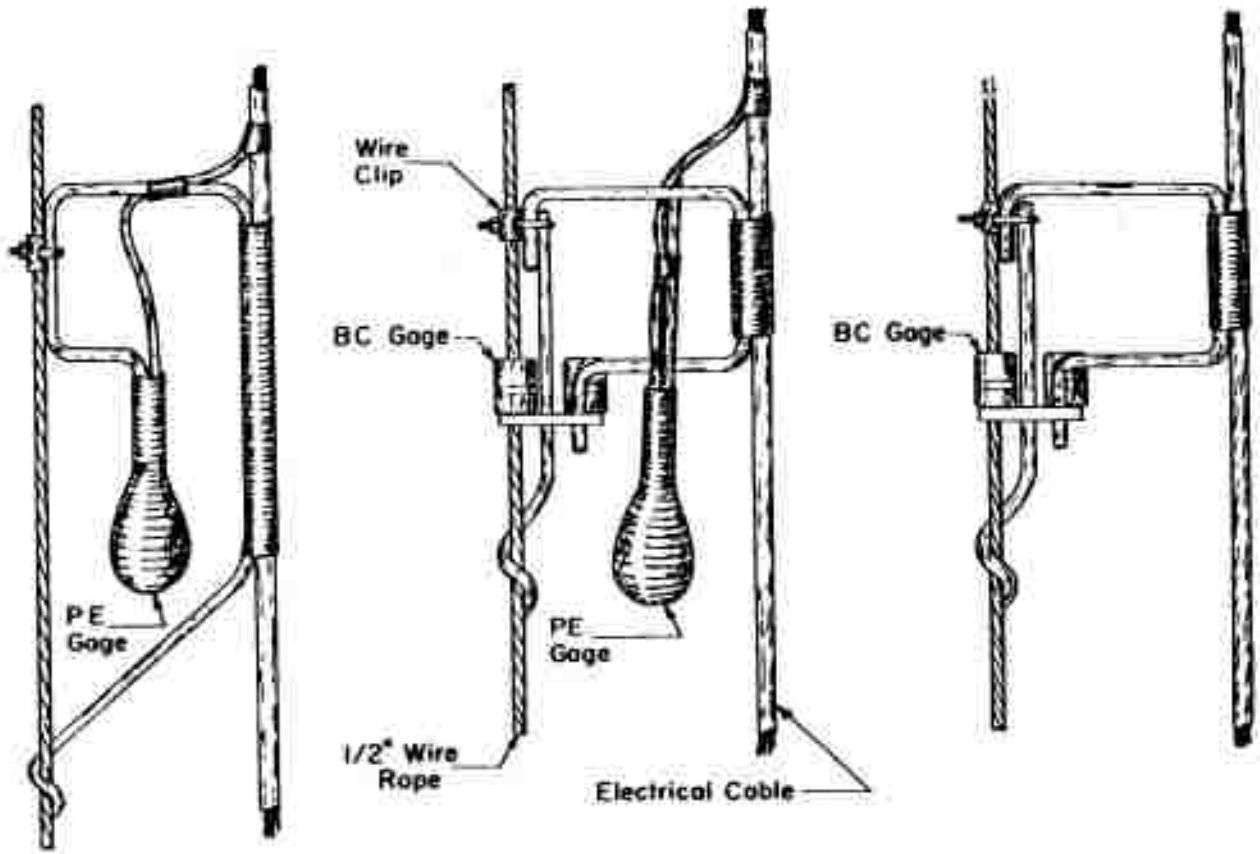

Figure 2.9 **Installation of PE and BC gages.**

CHAPTER 3

RESULTS

All of the five electronic recorders functioned and were recovered. Table 3.1 indicates the quality of record obtained from each electronic gage. Ninety-seven percent of the EPT gages yielded some information. The cutting of the gage string at Station 4 and the dropping of the recorder at Station 2 caused most of the loss of data. The reason for loss of the fiducial signal at Station 4 is unknown; the early fiducial signal at Station 3 was caused by one of many spurious signals generated there.

Ninety-one percent of the BC gage records were usable. Small deformations on most of the remainder were attributed to water leakage.

3.1 RECORDS AND MEASUREMENTS

Figure 3.1 illustrates the type of record obtained from the EPT gages at locations where refraction or anomalous surface cutoff did not obviously distort the wave shape. The particular record shown was obtained at Station 3 at the 2,000-foot depth. Figure 3.2 illustrates a record obtained at a location, Station 4, at the 982-foot depth, where refraction obviously affected the amplitude and wave shape.

Times, T, and pressures, P, were measured at or near

points designated E_1, E_2, etc., in Figures 3.1 and 3.2. The various events were identified as follows:

E_1 = direct shock wave arrival

E_m = maximum shock wave pressure, if different from E_1

E_2 = beginning of surface reflection wave front

E_3 = end of surface reflection wave front

E_4 = beginning of cavitation pulse

E_5 = surface reflection of E_4

E_6 = beginning of bottom reflection

E_7 = a major peak in the bottom reflection

E_8 = surface reflection of E_7

E_9, E_{10} —other events (See discussion, Section 4.5.)

3.1.1 Event Time on EPT Records. Arrival times were measured using the 360-cps time base and relative to the fiducial mark, or, in its absence, a shock wave arrival on a specified channel. The composite error from station to station in the recording of the fiducial signal was estimated to be less than 0.1 msec. Furthermore, the difference from one time base to another was estimated to be less than 1.5 msec over a period of 10 seconds. Each time base was calibrated, and these calibrations were used in computing the arrival times shown in Table 3.2.

Since event times were measured on the Visicorder records, and all data channels were played back simultaneously, identification of certain pressure pulses from channel to channel

was relatively easy. On the other hand, some pulses were of such low amplitude and of such slowly changing pressure that positive identification was difficult.

3.1.2 Pressure Measurements, BC Gages. The copper spheres from the BC gages were measured two or three times. At San Diego, they were measured either with micrometer calipers or with a special depth gage micrometer and jig. At NOL, the balls were remeasured once or twice using micrometer calipers. The results of these measurements are given in Tables 3.3, 3.4, and 3.5.

Station 1 measurements are recorded under F, the distance between flats. The deformation used in calculating the pressure is the ball diameter minus F and is recorded as X_m. Where all F values at one depth were about the same, they were averaged and a single value entered. Since all three balls from a given depth were stored in a single envelope, it was frequently impossible to match San Diego and NOL readings accurately. Where F values could be paired, and obvious differences in level existed, the average X_m for each ball was recorded.

Station 2 measurements made at San Diego were recorded directly as X, the deformation read with the depth micrometer. Measurements from San Diego and NOL were treated as at Station 1 to obtain pressure values.

Station 3 deformation measurements made at San Diego were recorded only to the nearest 0.001 inch and thus were

not of sufficient accuracy for use in this report. Only the NOL measurements are reported; they generally agreed with the San Diego measurements.

Using X_m, either average or individual, the value of K_d for use in Equation 2.1 was determined from Figure 2.3. The initial deformation X_o, and the hydrostatic pressure correction, P_o, for each depth were determined from Figure 2.4. The peak pressure was then calculated using Equation 2.1 and recorded as P_{ind} (for individual readings) or as P_{ave} for all three balls as a group.

Some individual values are not reported; the very small deformations indicated that water had leaked into the gage and prevented normal piston travel. Where the individual values showed large scatter, some discrimination in averaging seemed advisable. At depths of 125, 150, and 250 feet on Station 1, one or more of the three balls showed very large deformations. Since at most depths the hydrostatic pressure was sufficient to press the piston-ball-anvil assembly tightly together, excess deformation due to impact loading (analogous to piston retaining spring failure at shallow depths) was considered unlikely. For reasons explained in Section 4.3, the large deformations are believed to represent real pressure pulses. The value favored where large values occur is indicated (1). If two values are favored, they are marked (2) and their average given below the average for all three spheres.

3.1.3 Pressure Measurements, Electronically Recorded.

The non-linear gage calibrations were used in computing shock wave pressures in two ways. All pressures on a record were first calculated using the process described in Section 2.2.6. Then the resulting shock wave peak pressure was used to determine the gage calibration, and this value was used as a constant to recalculate all subsequent pressure values. Values calculated using the first method are labeled "variable calibration" in this report; those calculated using the second method are labeled "fixed calibration". The latter values are analogous to values that would be obtained by using dynamic shots at the exact pressure developed by the Sword Fish shot peak pressures to determine a constant gage KA. Thus, this process approximates the one used on Wigwam (Reference 2) and Hardtack (Reference 5); and pressures, other parameters, and yields derived using the "fixed calibration" are comparable to those from other nuclear explosions. Since the effects of gage apparent nonlinearity on pressure measurements have not been resolved, some Sword Fish data is reported using both methods of calibration.

All the reported pressures are overpressures relative to the hydrostatic pressure at the gage depth. Bottom reflection pressures are reported relative to the apparent ambient pressure just prior to the pulse arrival. This method of measuring was considered desirable because either residual pressures from the direct shock wave or bubble,

instrument drift, or gage hysteresis sometimes caused an appreciable shift in the record base line from the position prior to shock wave arrival.

Peak pressure, P_1, pressure at start-of-cutoff, P_2, and pressure at the end-of-cutoff, P_3, at the positions where the shock wave had a more or less exponential shape are given in Table 3.6. For other positions, the maximum shock wave pressure, P_m, and the time, t_m, of the maximum after initial shock arrival are given. Also given are the maximum pressures measured in the cavitation pulse, P_{4-5}, and the bottom reflection, P_{6max}. Where the peak pressure of the exponential shock wave was obtained by extrapolation of the semilogarithmic function back to zero time, it is denoted as P_{max}.

Considering the uncertainties in the gage calibrations and other instrumental accuracies, it is estimated that shock wave peak pressures are probably accurate to about ± 15 percent, while pressures at cutoff and in bottom reflections are only accurate to about ± 50 percent.

3.1.4 Time Constant, θ. The time constant, θ, is the time at which the presumably exponentially decaying pressure behind the shock front falls to 1/e of its initial value. Values of θ reported here are given in seconds. On Sword Fish, at most gage locations, the recorded decay was not exactly exponential. At some positions, refraction effects are believed to have been observed; at most positions, gage nonlinearity, or attempted corrections for it, are believed

to have affected the data. Where distortion of the shock wave was excessive, θ was meaningless.

Semilog plots of pressure versus time were made. Least square fits to increasing numbers of data points were performed by hand computations until the time to the last data point was greater than the resulting θ. Where cutoff arrived before θ, θ was found by a least squares fit to the data available prior to arrival of the cutoff wave. The results of these calculations, using both "fixed" and "variable" gage calibrations (see Section 3.1.3) are given in Table 3.7.

θ was also derived from machine-digitized pressure-time recordings, using a computer program to calculate θ and also the peak pressure, P_1, by extrapolation of the best computed fit to the pressure-time curve (see Section 2.2.7). These values are also shown in Table 3.7.

3.1.5 Impulse and Energy Flux Measurements. The integral of pressure as a function of time (impulse, I, psi-second) and the integral of pressure squared (multiplied by the factor ρc) as a function of time (energy, E, in-lb /in^2) was calculated to each measured point in a pressure pulse from the beginning of the pulse.

At some times during pulses showing multiple arrivals, negative pressures relative to hydrostatic were observed. During the negative phases, impulse and energy decreased; during the subsequent positive phase, they again increased, and so on. For the bottom reflections in particular, this

measurement was rather unsatisfactory, because base line drift caused large accruals which may or may not have been real.

Since the integration of the direct shock wave could not be carried out to 6.7θ, as is often done for high-explosive measurements, values are reported to 1θ, where available, and also at cutoff. The energy and impulse data are given in Table 3.8.

3.2 DATA FROM OTHER PROJECTS

Certain hydrographic and photographic data had been requested by this project as part of the support requirements. This information is considered to be basic to an accurate interpretation of the records obtained by this project and is summarized here.

3.2.1 Photographic Data. Results of the analysis of photographs indicate that the true surface zero was far beyond the target float. The positions of the various gage strings away from Station 1, relative to the target as deduced from Project 1.2 photographs (Reference 13), are given in Table 3.9. This information was combined with information derived from arrival times in making Figure 2.2.

3.2.2 Shock Wave Arrival Times. The time of arrival of the shock wave, relative to launch time, was obtained by Project 3.1 velocity meters at pertinent locations (Reference 14). This information is given in Table 3.10.

3.2.3 Hydrographic Data. Bathythermographs (BT) operated by naval ships and salinity-temperature-depth measurements by oceanographic vessels provided data on the acoustic properties in the ocean around the Sword Fish site. The information pertinent to the region in which pressure measurements were made is summarized in a sound velocity-versus-depth graph (Figure 3.3) and Table 3.11. This data is consistent with data given in Reference 15.

Bottom profiles were obtained by fathometers and from charts. The bottom in the region of project interest was found to be approximately level and at a depth of about 13,200 feet.

TABLE 3.1 SUMMARY OF SWORD FISH RECORDINGS.

Internal timing on all recorders satisfactory. a, spurious fuducial signals received; b, no fiducial signal received; x, satisfactory.

Station	Recorder	Depth	Channel	Fiducial	Pressure Calibration	Wave Shape	Arrival Time	Comments
		feet						
1	7	50	1	x	x	x	x	
		375	7	x	x	x	x	
		700	2	x	x	x	x	
		1,025	8	x	x	x	x	
		1,350	3	x	x	x	x	
		1,675	9	x	x	x	x	
		1,995	4	x	x	x	x	
2	12	50	1	x		x	x	
		375	7	x	x	x	x	
		700	2	x	x	x	x	
		1,025	8	x	x		x	Leaky gage
		1,350	3	x	x			No signal
		1,675	9	x	x	x	x	
		1,995	4	x	x	x	x	
3	17	25	1	a	x	x		
		50	7	a	x	x		
		375	2	a	x	x		
		700	8	a	x	x		
		1,025	3	a	x	x		
		1,350	9	a	x	x		
		1,675	4	a	x	x		
		2,000	10	a	x	x		

TABLE 3.1 (Continued)

Station	Recorder	Depth	Channel	Fiducial	Pressure Calibration	Wave Shape	Arrival Time	Comments
		feet						
4	5	25	1	b	x	x	x	
		50	7	b	x	x	x	
		375	2	b	x	x	x	
		700	8	b	x	x	x	
		982	3	b	x		x	Leaky circuit
		1,307	9	b	x		x	Leaky circuit
		1,632	4	b	x		x	Leaky circuit
		1,957	10	b	x		x	Hydrophone hysteresis
5	9	20	1	x	x	x	x	
		30	7	x	x	x	x	
		40	8	x	x	x	x	
		50	2	x	x	x	x	
6	Sony	200	1	x			x	

Pages 77 through 99 deleted.

TABLE 3.9 LOCATION OF GAGE STRINGS RELATIVE TO SURFACE ZERO AT TIME OF BURST FROM PHOTOGRAPHIC MEASUREMENTS.

Gage String	Ship	Bearing	Distance
		°true	feet
Station 1	Platform 2	332.0	3,120
Station 2	Platform 1	334.9	4,280
Station 3	USS BAUSELL	338.2	6,460
Station 4	USS MOLALA	338.	19,100
Station 6	USS MONTICELLO	252	23,600

Page 101 deleted.

TABLE 3.11 DEPTH VERSUS COMPUTED SOUND VELOCITY.

Depth	Velocity	Depth	Velocity	Depth	Velocity	Depth	Velocity
feet	ft/sec	feet	ft/sec	feet	ft/sec	feet	ft/sec
0	4,954.6	260	4,935.6	738	4,875.9	2,460	4,858.5
20	4,954.7	280	4,934.1	820	4,871.7	2,591	4,858.7
40	4,953.8	300	4,932.7	902	4,868.8	2,995	4,860.5
60	4,951.4	320	4,930.0	984	4,866.4	3,503	4,864.1
80	4,950.8	340	4,928.4	1,066	4,864.3	4,045	4,867.7
100	4,950.9	360	4,926.0	1,148	4,863.3	4,580	4,872.3
120	4,950.6	380	4,923.2	1,312	4,861.9	5,252	4,878.4
140	4,950.6	400	4,919.5	1,476	4,862.2	6,066	4,887.5
160	4,948.2	420	4,914.0	1,640	4,861.1	6,883	4,898.0
180	4,941.0	440	4,910.4	1,804	4,857.9	9,842	4,943.4
200	4,938.1	460	4,906.9	1,968	4,856.1	11,482	4,970.7
220	4,937.3	574	4,895.2	2,132	4,856.8	13,123	4,999.1
240	4,936.7	656	4,882.1	2,296	4,858.0	13,300	5,002.0

Pages 103 and 104 deleted.

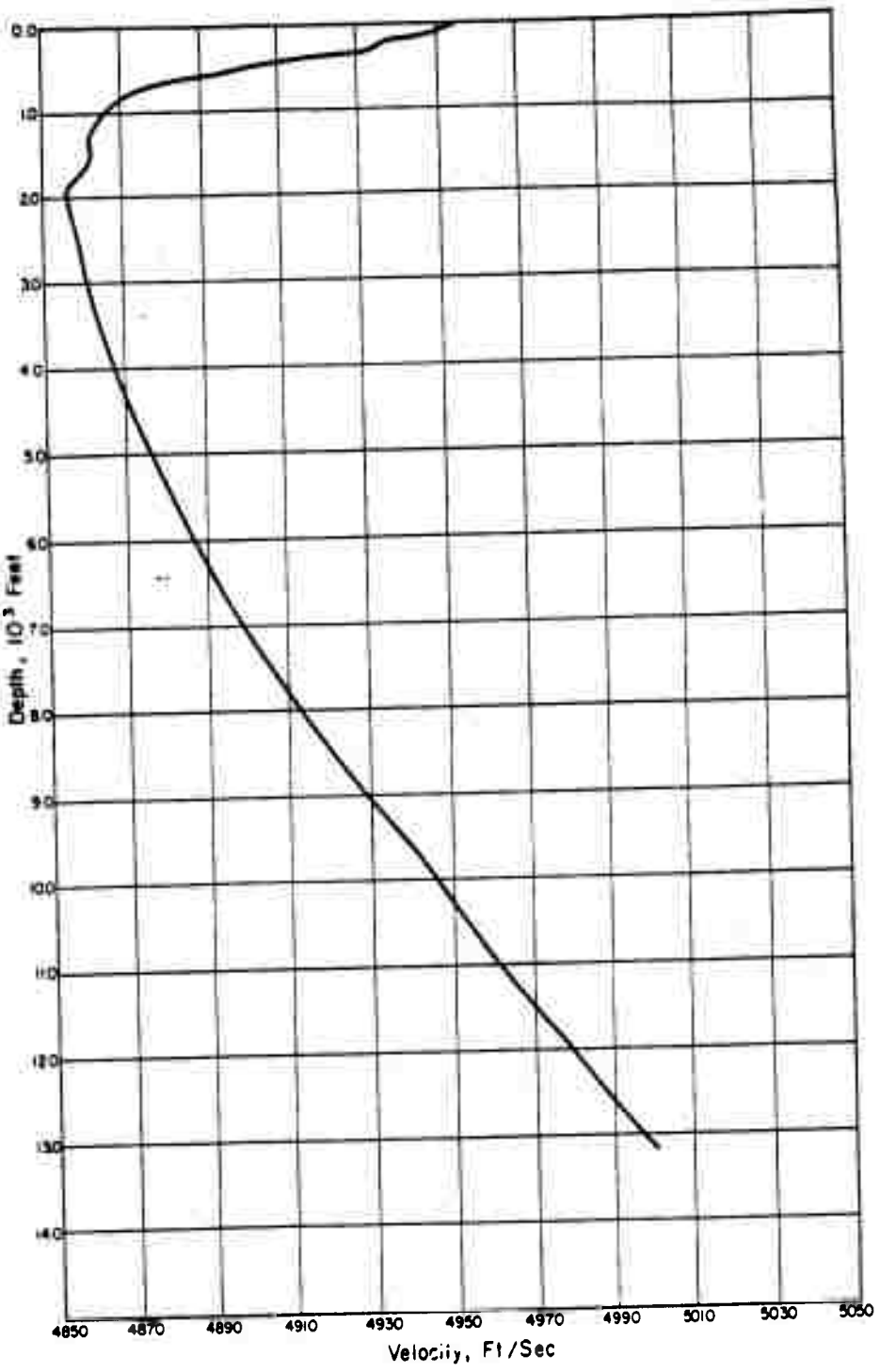

Figure 3.3 Sound velocity versus depth at test site.

CHAPTER 4

DISCUSSION

4.1 LOCATION OF BURST

The method chosen to determine the depth of burst was a refinement of the shock wave ranging system used on Wigwam to check the depth of burst and locate the bubble pulse (Reference 2). The method requires knowledge of the gage positioning, sound velocity structure of the water, yield of the weapon, range of the gage string, etc.

The raw data was the arrival time of the shock wave at various gages (Table 3.2), particularly those at Station 1, and the sound velocity structure near the test site (Table 3.11). Though it is possible to determine the range from the arrival time data, it is believed that the aerial photographs provided a better figure, at least for Station 1.

Using the machine computation program described in Chapter 2, an initial set of calculations was made for several yields and a chosen range of depths of burst. The gage array was assumed to be vertical. Each gage provided two data points: the initial arrival and the termination of the surface cutoff (reflection) phenomena. The beginning of cutoff occurs prior to the acoustic approximation prediction

because of high amplitude effects ("anomalous cutoff") occurring at free-surface reflection (References 6, 16, and 17). The surface reflection provides an image source which may be used to determine deviation from the vertical and curvature of the gage line.

In order to make a quantitative measurement of the quality of fit of the calculated to observed data, the following equation was used:

$$\Delta T = (T_{ra} - T_{ga}) - (T_{rc} - T_{gc}) \qquad (4.1)$$

Where for Stations 1 and 2:

ΔT = difference between calculated and measured arrival times, seconds

T_{ra} = arrival time at reference gage (1,995-foot depth) from Table 3.2, seconds relative to fiducial signal

T_{ga} = T_1 or T_3 from Table 3.2, depending on whether real or image position for a gage, seconds relative to fiducial signal

T_{rc} = computed travel time to reference gage, seconds

T_{gc} = computed travel time to the other gage, seconds

And for Station 3:

T_{ra} = arrival time at reference gage (2,000-foot depth) from Table 3.2, seconds after first arrival at 375-foot gage

T_{ga} = T_1 or T_3 from Table 3.2, depending on whether real or image position for a gage, seconds after first arrival at 375-foot gage

Minor errors in gage placement or computation could greatly affect ΔT for any individual gage. By use of data from groups of gages, the effects of individual errors were reduced. Using mirrored groups (for example, the lowest six real gage positions and the top six image gage positions), the average ΔT for each group was obtained. Then, using the method of least squares, a line was fitted to the gage depth versus ΔT data for each group. The lines' slope and intercept with the ΔT axis were determined.

In an ideal case (i.e., the gage line vertical and straight, a perfectly known velocity structure, etc.), at only one depth of burst would the average ΔT's for image and real gage groups and the slopes of the fitted lines be zero and the intercepts of the slopes occur at $\Delta T = 0$. It was found that when any criterion for a group of either image or real gages was zero for a certain depth burst, the same criterion for the congruent set was not zero. Realizing that the array was probably not stationary in the water, assumption of a slant in the gage line was made, and new calculations were made for arrival times at different depths of burst, etc. A positive slant of the array showed as an increase of the horizontal range of the gages as one moved away from the

surface, either up into the image array or downward into the real array.

It was found after calculating for several slants (Table 4.1) that there was a nearly linear relationship between the slant and the depth of burst as determined by the parameters (zero slope, zero ΔT, or zero intercept of slope) for individual gage groups. The array slant (in minutes) at which each parameter became zero for congruent groups and the depth of burst were calculated, and the results are given in Table 4.2.

The individual ΔT data for the gage nearest the surface usually deviated more from the fitted line than did the ΔT data calculated for the other gages. In an attempt to remove this larger deviation, calculations were made without using data from the near-surface gage or gages. Comparing Tables 4.1 and 4.2, it is seen that this did not improve the situation much.

Finally, calculations were made for Station 1 assuming that the two gages nearest the surface were on a vertical line and that a line through the other gages slanted away from the burst. The scatter of the average depth of burst as determined by the three parameters was least for this assumed geometry but was still within the values obtained using the straight, slanted array.

Considering the straight, slanted array values, it is to be noted that, though the slants are not the same, all are in the same direction and within about one standard deviation of one another. Scatter of the depth of burst and slants is attributed to a combination of errors in calculation of the shock velocity, errors in range of the stations, and individual errors in gage positioning, both vertically along the support cable and transversely from the geometric straight line.

After the above computations were completed, the various machine programs were consolidated and minor errors of method corrected. The consolidated program assumed that the operator knew the range to the top of a gage line, the yield, and a velocity structure. The raw data was the direct wave arrival time and cutoff time at the gages. The program assumed in its first approximation that the explosion was at zero depth and the gage line was vertical. It then postulated bracketing depths of burst and gage line slant, computed arrival times for the four cases, computed differences, fitted lines to difference-versus-depth relationships, and solved for the three depths of burst and array slants at which intercepts, averages, and slopes were zero. Then it averaged the results and calculated the mean deviations.

Using this new depth of burst and slope, the program selected new bracketing conditions slightly closer to the

average values just found. It repeated the computation for a preselected number of trials. After a few trials, relatively constant values of depth and slant were attained.

The results of the final machine computations are given in Table 4.3. They do not agree too well with the values given in Tables 4.1 and 4.2, possibly because of revisions in the computation process or because of the choice of more appropriate slants and depths of burst in making the approximations. Typical results from the preliminary and final computations are plotted in Figure 4.1. A large effect of range of the recording station on the depth of burst determination in the final computations seems evident; this is attributed to noninclusion of refractive bending of paths. Refractive effects tend to decrease the calculated depth of burst; some effect would be expected even at Station 1.

4.2 TIME OF BURST

Launch occurred at 1301:26.1004 local time (Reference 18). The first fiducial pulse was transmitted at 1302:01.5812

local time at the Sword Fish site. The shock wave arrived at Station 1 at the 50-foot-deep gage after the fiducial signal.

Assuming and a yield from the time for the shock wave to travel from the burst point to the 50-foot-deep gage at Station 1 (3,120- ± 10-foot horizontal range) was calculated to be second. Rounding slightly, the burst time is then 1302:05.909 ± 0.005 second local time or 2002:05.909 ± 0.005 Greenwich mean time, 11 May 1962. This is 39.809 seconds after launch.

4.3 REFRACTION EFFECTS

Refraction had several effects on the results obtained and the way in which they were used. It changed the shock wave pressure and thus the energy input to the target vessels. It changed the travel time of the shock wave to gages and thus the use of arrival times in calculating the depth of burst (see Section 4.1). The extent of the region in which anomalous surface cutoff (Reference 16) occurred was probably affected by ray bending near the ocean surface. Shadow zones, and probably caustics, were formed.

The effects on the shock wave pressure-time curve were most obvious at Station 4 where the wave shape was greatly distorted At Station 3, the wave shape was somewhat distorted at the

Even at Station 1 at the 375-foot depth, there is an indication of distortion. Of course, a general increase or decrease of the pressure level at any gage could have been caused by refraction without changing the wave form; such an effect could not be differentiated from gage calibration error.

The ball crusher gage pressure measurements were plotted (Figure 4.2) as a function of depth at each of three stations. Some electronic gage peak pressures are also shown on Figure 4.2. It is at once clear that the pressure versus depth is not a smooth function. The deviations from smooth curves that might be drawn through the data points are caused by a combination of refraction effects and instrumental errors.

A computer program previously developed to make refraction effects predictions and the depth versus sound velocity data (Table 3.8) were used to make calculations of the sound intensity factor, F (F = 1/sound intensity), for the Sword Fish condition relative to F in isovelocity water.

A pattern of sound ray paths was also obtained (Figure 4.3). By cross plotting the intensity factors along the rays, it was possible to construct a pattern of lines of constant relative intensity factor (Figure 4.4). From this pattern, the graphs of intensity factor versus depth at Stations 1, 2, and 3 were drawn (Figure 4.5). Exact determination of the intensity factor in

regions of ray crossover does not seem to be feasible or worthwhile at present; therefore, the calculated intensity factors in and beyond such regions are approximate. The purpose of these calculations was to obtain factors by which the observed peak pressures could be divided to obtain theoretical isovelocity water peak pressure values.

Figures 4.3, 4.4, and 4.5 show that there should be thin layers of high and low relative intensities extending outward from surface zero. Though the relative intensity in a layer may vary with range, a single layer should be detectable at all three close-in stations. This is indeed the case (Figure 4.2). For example, the very high pressure recorded at the 125-foot depth at Station 1 (Table 3.3) is probably real. Two out of three BC gages indicated the higher pressure, but the evidence did not seem credible until the refraction calculations were complete. The calculations did not show as high a relative amplitude at Station 1 as at Station 3, but at all three stations, an increase in pressure was indicated near the 125-foot depth. It is because of this trend that this unusual BC data should be accepted.

The agreement between theoretical values and measured values is not very good, either in depth of layer or in pressure, but more than chance correspondence certainly exists. The agreement seems to decrease with greater range; observed pressures seem to indicate relatively less refraction effect

at greater ranges than predicted. The real effects are still large.

Though the refraction effect study was interesting and probably explains some of the unusual pressure values reported, it is not sufficiently quantitative (or accurate) to assist in determining the yield. Refraction theory did not in this case give valid correction factors for the measured peak pressure values, possibly because of inadequate input data.

4.4 YIELD CALCULATIONS

The yield of the weapon based on hydrodynamic measurements and standards determined using Wigwam data (References 2 and 12) was calculated using the EPT and BC measurements made at Stations 1, 2, and 3. Equations 2, 3, 7, and 8 given in Reference 12 were rearranged (and Equations 7 and 8 modified for use out to only one time constant, θ) as follows:

$$\log Q = \frac{\log P + 1.13 \log R - 6.64147}{0.3767} \qquad (4.2)$$

$$\log Q = \frac{\log \theta - 0.22 \log R - 0.35679}{0.26} \qquad (4.3)$$

$$\log Q = \frac{\log I + 0.91 \log R - 3.79906}{0.6367} \qquad (4.4)$$

$$\log Q = \frac{\log E + 2.04 \log R - 9.72556}{1.013} \qquad (4.5)$$

Where: Q = yield, kilotons

R = slant range, feet

P = P(ball crusher) or P_{max}(extrapolated peak pressure of pseudo-exponentially decaying shock wave), psi

θ = time constant, milliseconds

I = impulse, psi-sec, integrated to 1θ

E = energy flux, in-lb/in^2, integrated to 1θ

The reason for using data out to only one time constant was that the shock wave duration is limited by surface cutoff.

Most data points available for comparison of the nuclear shots include information out to 1θ; at very shallow gage positions, cutoff occurred even earlier. Furthermore, the exponential decay constant increases more rapidly after 1θ. In other words, the shock wave decays approximately exponentially out to 1θ; thereafter it decays more slowly. The data after 1θ are of value, but not for yield determination.

Using Equation 4.2 and ball crusher gage peak pressures from Tables 3.3, 3.4, and 3.5, Table 4.4 was compiled. Figure 4.5 shows that small displacements in depth of the layers may compound the refraction corrections and should thus vary the calculated yield excessively. Despite this, some calculations were made; the results were as expected and are not

reported.

Using the piezoelectric pressure time data from Tables 3.6, 3.7, and 3.8 and Equations 4.2, 4.3, 4.4, and 4.5, Tables 4.5 and 4.6 were compiled. In Table 4.5, the results of manual measurement followed by machine computation are given. In Table 4.6, the results of machine reading and analysis are given (see Section 2.2.7). At each gage position, the yield was calculated by all the equations except where cutoff or superimposed timing marks prevented determining impulse and energy to 1 θ. Yields calculated from two or four parameters at each gage position were averaged. All yields obtained for each parameter at each station were averaged. All yields at each station were averaged. All yields from three stations were averaged. Finally, all yields from Stations 1 and 2 were averaged. Tables 4.5 and 4.6 show no clear cut superiority of the machine analysis; for some combinations of results, the hand analysis gives a smaller standard deviation. But for Station 2, the yield is brought close to that for Station 1 and the standard deviation to a relatively very low value. It is believed that this is a result of the more accurate determination of θ, which of course affects both impulse and energy measurements to 1 θ.

Only raw data with no correction for refraction gave the yields in Table 4.4. Many of the BC gages were in regions where the peak pressure was generally reduced by refraction

effects. Where BC gages and PE gages were paired, the BC values were generally lower than PE values. When average BC and PE peak pressure yields are compared (Tables 4.4 through 4.6), the same trend of smaller BC value is evident. A slight trend of apparent increase in yield with increasing range for both types of gage is also evident.

Since most past comparisons of chemical and nuclear explosions leaned heavily on PE data, somewhat more weight is given to the PE values in selecting a single yield value for Sword Fish. Averaging of yields from the four parameters, P_{max}, θ, I, and $\bar{E}$, tends to smooth the effect of low peak pressure coupled with long time constant such as was measured at the Station 1, 700-foot-depth position. There are many factors affecting the PE results: gage calibration, gage size effects, and nonlinearity of system response. At low pressures such as were observed at Station 3, these factors tend to give a high reading of pressure. Station 3's higher yield value may have been caused by refraction and this system error working together. The average individual yield values for Stations 1 and 2 have low scatter, as the data are less affected by refraction, and the secondary gage calibration effects are less at higher pressures. Therefore, the average of the machine analysis values from Stations 1 and 2 has been selected as the best underwater shock wave measure for Sword Fish. This yield value is

4.5 OTHER PHENOMENA

Surface cutoff at all deep, close-in gages was regular; that is, the reflected wave caused a rapid, linear decrease in pressure as shown at the bottom of Figure 3.1 between T_2 and T_3. Since the Wigwam and Wahoo cutoff times agreed well with theoretical predictions, cutoff times were used in Section 4.1 to aid in the determination of the depth of burst. No calculations concerning the theoretical rate of decrease in pressure nor of the negative wave velocity as affected by its propagation through the tail of the shock wave were made.

The shape of the cutoff wave agreed qualitatively with that expected. At Stations 1 and 2, there was no evidence of anomalous cutoff; none of the slanting part of the negative wave front reached the shock front.

At Station 3, there may have been anomalous cutoff, but it is not possible to determine this from the shape of the shock wave because of the long rise time of the recording system which distorts short pulses. The record obtained at 50 feet can be extrapolated back to correct for system response. This gives a peak pressure value essentially in agreement with the free water value; hence, anomalous cutoff has had negligible effect here. The record at 25 feet, however, gives too low a value with any reasonable extrapolation; anomalous cutoff probably occurred at this depth.

At Station 5, anomalous cutoff apparently occurred at

all four gage depths. At Station 4, the shallow gages were in a definite shadow zone, and no regular cutoff occurred. Though the deepest gages failed to record properly, the one at 1,957-foot depth indicated a regular shock wave arrival.

A group of pressure waves reflected from the bottom of the ocean and underlying layers of denser rock was observed at all stations. The first arrival time (T_6 in Table 3.2) measured at each station relative to the shock wave arrival indicated the bottom depths listed in Table 4.7. A large peak in the pressure waves was measured at Stations 3 and 4, and its arrival time (T_7 in Table 3.2) indicated a good reflecting layer (subbottom) at depths also shown in Table 4.7. (A sound velocity of 11,400 ft/sec was assumed in the ocean bottom sediments.)

A second group of waves that had traveled from the burst to the bottom, thence to the surface, to the bottom, and then to the gage, was observed at Stations 3, 4, 5, and 6 (later pulse in Table 3.2). The bottom and subbottom depths postulated on the basis of arrival times from the second bottom reflections are also given in Table 4.7.

In both groups of reflections, the rearrival of some of the pulses after reflection from the surface after passing the gage was detectable at some positions (T_8 in Table 3.2 for the first subbottom reflection).

The data from Table 4.7 were averaged. It appears that

the ocean bottom was at a depth of about 13,400 feet with a main reflecting layer at a depth of about 17,000 feet. The bottom depth indicated is about 200 feet greater than previously reported (Reference 18). It is possible that Project 1.1 did not detect reflections from the soft clay bottom but only from harder underlying rock layers, the first of which may have occurred according to Reference 18 at 13,340 ± 60 feet.

The peak pressure of a shock wave that traveled a free-water path equal in length to that of the bottom reflection was calculated for selected gage positions. The calculated peak pressures are compared with the measured values of the bottom reflection in Table 4.8 and the ratio of the pressure of the reflected wave to that of the free-water path (bottom reflection coefficient) tabulated.

It is apparent that the method of reading the analog record determines the absolute pressure in the bottom reflections. This is because of the way the ramp calibration is interpreted in hand and machine record analysis. In reading by hand, gear noise may be interpreted as a change in calibration, but actual values measured on the calibration ramp are used. When analyzed by machine, the gear noise is suppressed in an averaging process, but negative ramp deflections are obtained by backward extrapolation. As a result, the hand values may be more nearly correct on an absolute scale but

less accurate because of noise.

The reflections from the deep layer(s) are definitely stronger than the first arrival. No strong trend of bottom reflection coefficient with increasing horizontal range is discernible. From the pressure data and the bathymetric-geological data available, it is impossible to draw any conclusions concerning the magnitude of the bottom reflection coefficient, its dependence on bottom composition, the effects of focusing, or the effect of pulse amplitude on the coefficient.

Measurements of bottom reflection impulse and energy were not attempted at Stations 1, 2, and 3 because of record interpretation difficulties.

Project 3.1 (Reference 14) reported that the bottom reflection was more damaging to the target vessels than the direct shock wave. Project 1.1 results at Station 3 confirmed these conclusions. At Stations 4 and 6, the bottom reflection seemed to observers to be much more violent than the direct wave. Project 1.1 records at Stations 4, 5, and possibly 6 corroborated that observation.

Pages 123 through 137
deleted.

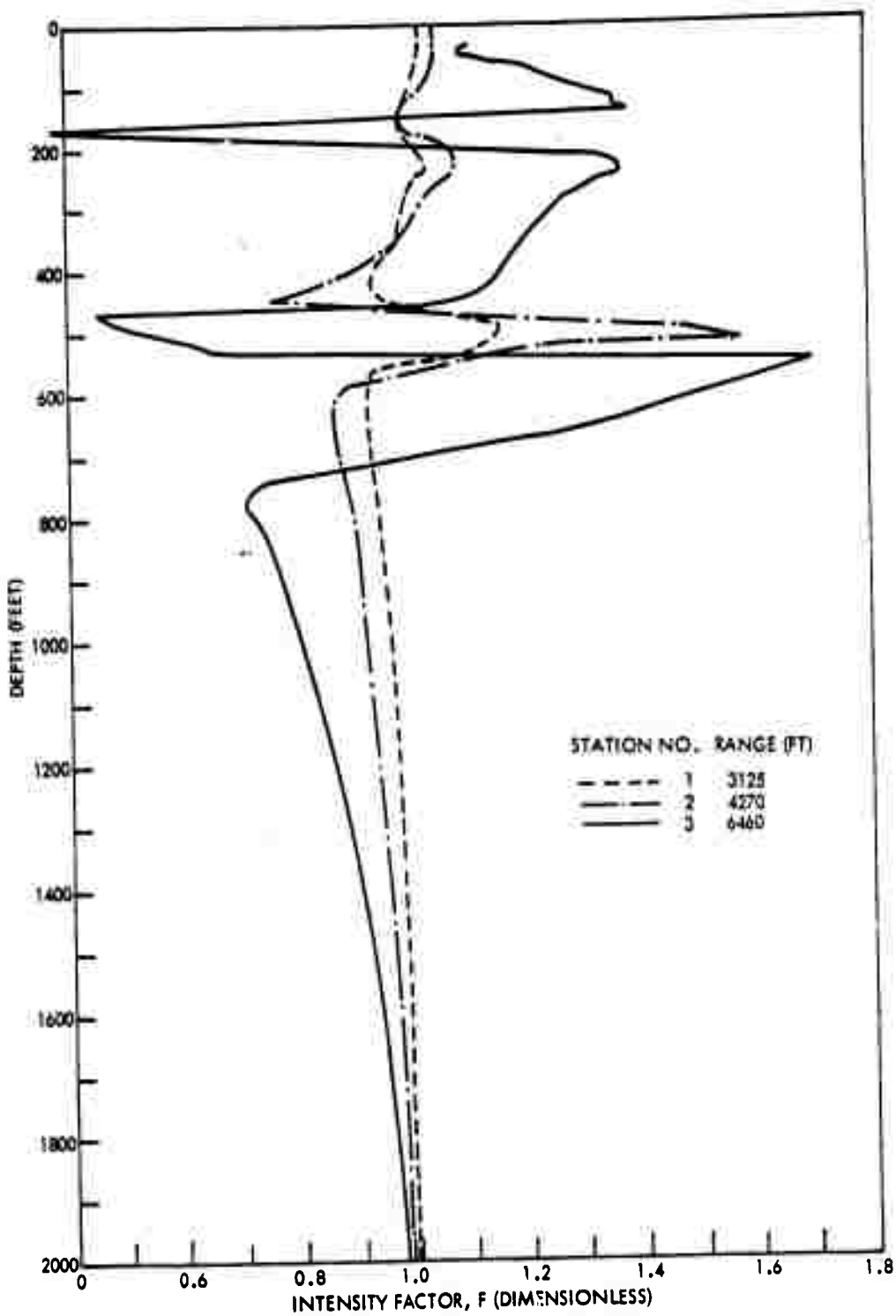

Figure 4.5 Intensity factor versus depth at three stations. (U)

CHAPTER 5

CONCLUSIONS

The results of the shot fired under the Sword Fish conditions of sound velocity profile, bottom depth, bottom composition, and entry trajectory were as follows:

1. The hydrodynamic yield was found to be equivalent to The depth of burst was The time of burst was 39.8095 ± 0.010 second after the launch zero time. The geographic surface zero position was not determined by this project but was about 3,120 feet from Platform 2 (project Station 1).

2. Refraction effects were detected in electronic pressure measurements to a depth of 450 feet at 4,200 feet standoff and to greater depths at larger standoffs. Refraction effects in mechanical measurements of peak pressures were observed as close as 3,120 feet.

3. The bottom reflection was more powerful than the direct shock wave at ranges of more than

4. No bubble pulse was detected at any range.

APPENDIX

MECHANICAL SHOCK MEASUREMENTS

Measurement of the peak shock experienced by Platforms 1 and 2, while not in the original Project 1.1 plan, was undertaken to provide data on future platform designs. The platforms used in the Sword Fish test are typical of those generally used in the lethal region of underwater explosions. (U) The shocks experienced by the platforms were considerably lower than those predicted and below the useful range of the accelerometers used. Nevertheless, information on how the accelerometers were used and what they yielded is presented for whatever value it may have in future tests.

A.1 NOL COPPER BALL ACCELEROMETERS

The copper ball accelerometer (Reference 19) is a self-recording mechanical device used to measure peak acceleration. NOL accelerometers are of two types: (1) the conventional type designed to record a single shock pulse, and (2) the discriminating type designed to record portions of complex or multiphase shocks. The NOL Mod 5 and Mod 6 accelerometers were used for the Sword Fish tests.

All accelerometers used on Sword Fish had shock-actuated discriminators that mechanically control recording time. The devices allow the accelerometers to record only for several

milliseconds during the initial shock. Recording time depends on the level of shock. Based on a predicted Station velocity change of 16 ft/sec, the Mod 5 accelerometer recording time would have been about 5.2 msec and the Mod 6 time about 3.9 msec. At Station 2, the predicted velocity change was 6 ft/sec. The corresponding recording time for the Mod 5 accelerometer would have been about 13.9 msec and the Mod 6 time about 10.4 msec. This discriminating feature was essential because several shocks were expected to occur in close time sequence during the test. Also, it insured that gear that may have broken loose during shock and crashed to the deck did not affect the accelerometer readings.

At Station 1, six accelerometers were used, covering a range of shock from about 200 to 20,000 g. At Station 2, two accelerometers covered a range of shock from 200 to 6,000 g. The natural frequency of the accelerometers ranged from 565 to 1,749 cps.

(U) A.2 ACCELEROMETER MOUNTS

The Station 1 accelerometers were mounted in an escape float; those at Station 2 were mounted directly to the deck. Figure A.1 shows schematically the escape float rig and identifies the location of the Station 2 accelerometers. The Station 1 platform was considered to be near the lethal range of the explosion, and there was some possibility it would sink. The escape float, made of hard pine, was secured

to the deck, clear of other gear, with a wire rope sling. The sling, shown in Figure A.1, included a turnbuckle and a MK 3 Mod 3 mine release. If the barge sank, the hydrostatic release was to free the sling and allow the float to rise to the surface. The accelerometers were mounted in the cavity of the float on an aluminum plate. The plate made up the bottom of the float and rested hard against a rigid member of the barge.

Page 143 deleted.

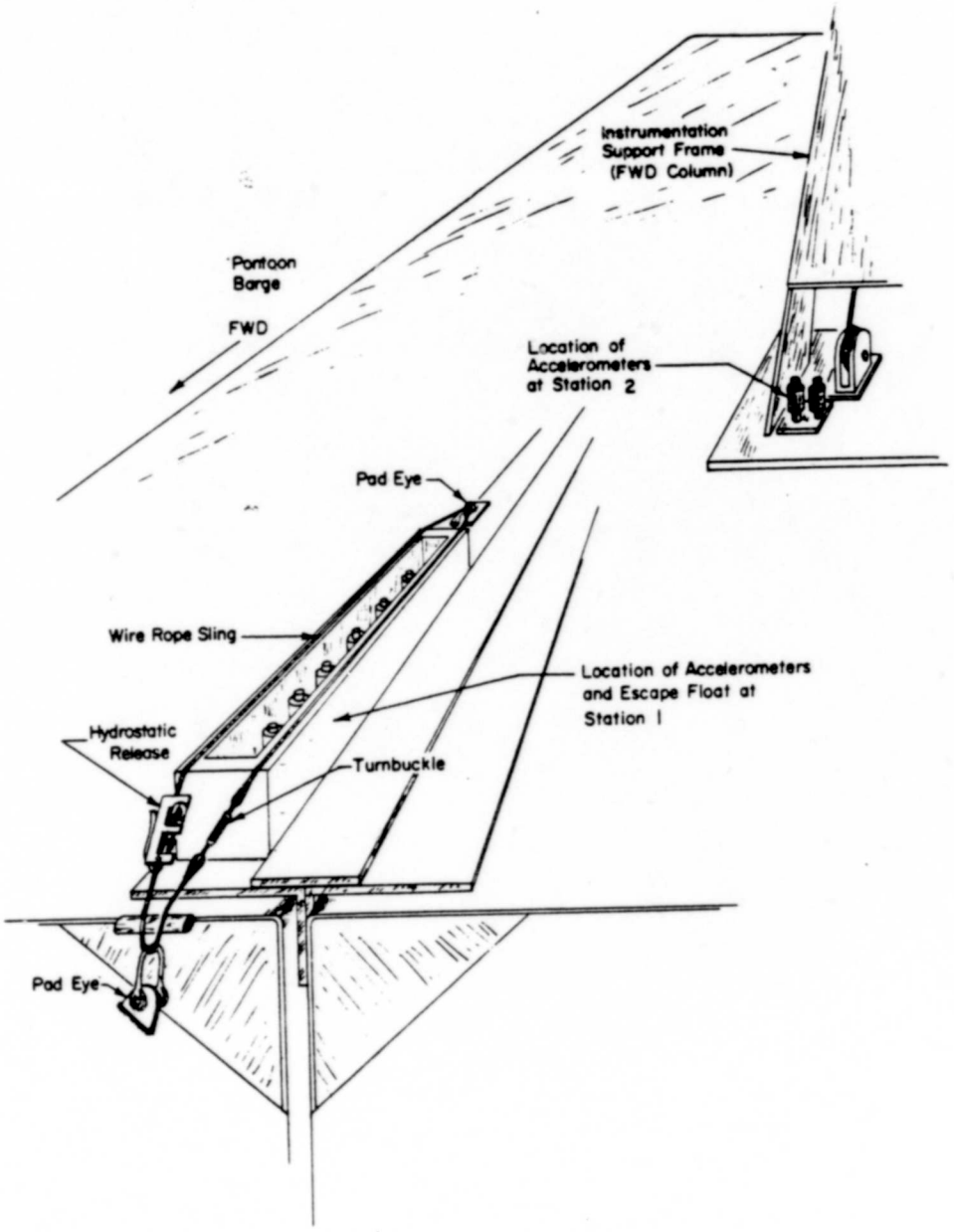

Figure A.1 Accelerometer arrangements.

REFERENCES

1. T. McMillian; "Underwater Free-Field Pressure Measurements"; Project 1.3, Operation Wigwam, WT-1007, May 1955; U. S. Navy Electronics Laboratory, San Diego 52, California; Confidential Formerly Restricted Data.

2. C. J. Aronson and others; "Underwater Free-Field Pressures to Just Beyond Target Locations"; Project 1.2, Operation Wigwam, WT-1005, May 1957; U. S. Naval Ordnance Laboratory, White Oak, Silver Spring, Maryland; Confidential Formerly Restricted Data.

3. C. B. Cunningham; "Free-Field Pressures, Station Zero"; Project 1.2.1, Operation Wigwam, WT-1006, May 1955; U. S. Naval Research Laboratory, Washington 25, D. C.; Confidential Formerly Restricted Data.

4. T. McMillian and others; "Refraction of Shock from a Deep-Water Burst"; Project 1.5, Operation Hardtack, WT-1610, October 1960; U. S. Navy Electronics Laboratory, San Diego 52, California; Confidential Formerly Restricted Data.

5. E. Swift, Jr. and others; "Underwater Pressures from Underwater Bursts"; Project 1.1, Operation Hardtack, WT-1606, August 1960; U. S. Naval Ordnance Laboratory, White Oak, Silver Spring, Maryland; Confidential Formerly Restricted Data.

6. (a) G. K. Hartmann and E. G. Hill, editors; "Underwater Explosion Research, Volume 1, The Shock Wave"; 1950; Office of Naval Research, Department of the Navy; Unclassified.

(b) J. S. Coles and others; "The Measurement of Underwater Explosions from Service Weapons at the Underwater Explosives Research Laboratory (UERL)"; NDRC Report A-362, OSRD Report 6240, March 1946; Unclassified.

7. C. R. Niffenegger and M. A. Thiel; "The Ball Crusher Gauge, Modified Gauge Designs, Predeformation and Waterproofing Tests (U)"; NAVORD Report 4224, 1 July 1956; U. S. Naval Ordnance Laboratory, White Oak, Silver Spring, Maryland; Confidential.

8. E. A. Christian and C. R. Niffenegger; "Piezoelectric Gages for Underwater Measurements, I. The Aging of Tourmaline Gages by Underwater Shock Waves"; NAVORD Report 2928, 15 July 1953; U. S. Naval Ordnance Laboratory, White Oak, Silver Spring, Maryland; Unclassified.

9. R. H. Cole; "Underwater Explosions"; 1948; Princeton University Press, Princeton, New Jersey; Unclassified.

10. V. S. Newton; "A Frequency Modulation Playback System with Wow and Flutter Compensation (U)"; NAVORD 6633, 1 August 1959; U. S. Naval Ordnance Laboratory, White Oak, Silver Spring, Maryland; Unclassified.

11. J. M. Richardson, A. B. Arons, and R. R. Halverson; "Hydrodynamic Properties of Sea Water at the Front of a Shock Wave"; The Journal of Chemical Physics, November 1947, Vol. 15, No. 11, Pages 785-794; Unclassified. (Or Reference 6(a)).

12. H. G. Snay and J. F. Butler; "Shock Wave Parameters for Nuclear Explosions Under Water"; NAVORD Report 4500, May 1957; U. S. Naval Ordnance Laboratory, White Oak, Silver Spring, Maryland; Confidential Formerly Restricted Data.

13. G. A. Young and D. E. Phillips; "Surface Phenomena (U)"; Project 1.2, Operation Dominic, Shot Sword Fish, POR-2001, 14 August 1964; U. S. Naval Ordnance Laboratory, White Oak, Silver Spring, Maryland; Secret Formerly Restricted Data.

14. C. M. Atkinson, W. E. Carr, R. E. Baker; "Studies of Shock Motions of Hull and Equipment (U)"; Project 3.1, Operation Dominic, Shot Sword Fish, POR-2005, 1963; David Taylor Model Basin, Washington 25, D. C.; Secret Formerly Restricted Data.

15. B. H. Ketchum, N. Corwin, and P. B. Stimson; "Oceanographic Observations During Operation Sword Fish (U)"; U. S. Atomic Energy Commission Report NYO-3008-1, October 1964; Woods Hole Oceanographic Institution, Woods Hole, Massachusetts; Confidential Restricted Data.

16. J. H. Rosenbaum and H. G. Snay; "On the Oblique Reflection of Underwater Shock Waves From a Free Surface I"; NAVORD Report 2710, 1 November 1956; U. S. Naval Ordnance Laboratory, White Oak, Silver Spring, Maryland; Unclassified.

17. J. H. Rosenbaum; "On the Oblique Reflection of Underwater Shock Waves From a Free Surface II (U)"; NAVORD Report 2855, 1 April 1953; U. S. Naval Ordnance Laboratory, White Oak, Silver Spring, Maryland; Confidential.

18. W. W. Murray; "Scientific Director's Summary Report (U)"; Operation Dominic, Shot Sword Fish, POR-2007 (WT-2007), 21 January 1963; David Taylor Model Basin, Washington 7, D. C.; Secret Restricted Data.

19. V. F. DeVost; "NOL Copper-Ball Accelerometers"; NAVORD Report 6925, 27 July 1960; U. S. Naval Ordnance Laboratory, White Oak, Silver Spring, Maryland; Unclassified.

Pages 149 through 154 deleted.